THOMAS CADENAZZI

UNIVERSITY OF MIAMI

STUDY OF AN EXPERIMENTAL ANCHOR SYSTEM – “STAPLE ANCHORS” - FOR EXTERNALLY BONDED FRP LAMINATES USED FOR THE CONSOLIDATION AND RETROFITTING OF REINFORCED CONCRETE STRUCTURES

Academic year: 2015/2016

TABLE OF CONTENTS

1. INTRODUCTION

This report investigates a new type of anchorage system, called “staple” anchor as a mean of anchoring externally bonded fiber-reinforced polymers (FRP) sheets into concrete. The investigation will employ experimental work, which includes concrete blocks strengthened with FRP sheets connected to the concrete blocks footings via these innovative types of carbon anchors set up in different configurations.

The staples anchors are designed in two different types: flat staples and round staples. Both the types of anchors are provided as prefabricated elements formed by strands of carbon fibers that are inserted into epoxy filled holes in the concrete, and an external part that is also impregnated and connected externally to the bonded FRP laminate. They appear in different shapes and sizes and they also have different processes of installation but they share the same aim: enhance the bond of externally bonded FRP laminates into concrete.

The experimental campaign is composed by a double shear test through which it is investigated the resistance of the anchors under tension load in different anchor configurations, in order to find the best configuration that is sufficient to enhance the bond of the FRP sheets. In particular, two series of double shear tests are performed: the first one is conducted with a past method already used in the University of Miami laboratory to investigate the performance of the spikes’ anchors. Since this past method revealed some difficulties in the set-up procedure of the test and mostly inaccurate results, a second test is performed with an innovative installation procedure and set-up of the test, which gives successful and consistency results through a more reliable set-up of the test.

The purpose of this report is to test the effectiveness of the flat staple anchors and to create new specific design guidelines, providing to engineers, in this way, the necessary information to make design decisions when incorporating a staple anchor system to enhance the bond of externally bonded FRP laminates. Finally, also a comparison between the performance of the spikes anchors’ type is provided.

1.1 Staples Anchorage system

In this section, we will not go much in too deep the process of the anchors' making and assembling. This section, though, describes, in general, the principal anchors' characteristics and the main differences between them, respecting in this way the will of the producer.

1.1.2 Flat staple

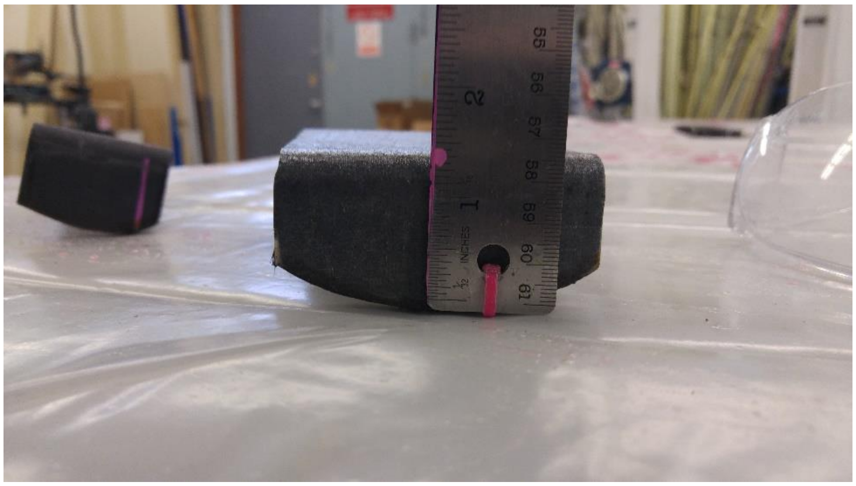

The flat staple anchors are called so thanks to their shape that literally recall the shape of a staple.

With the uni-directional fibers of the anchor aligned in a longitudinal way to the flexural FRP sheet, the flat staple anchor is made by carbon fibers pre-impregnated with a particular synthetic resin.

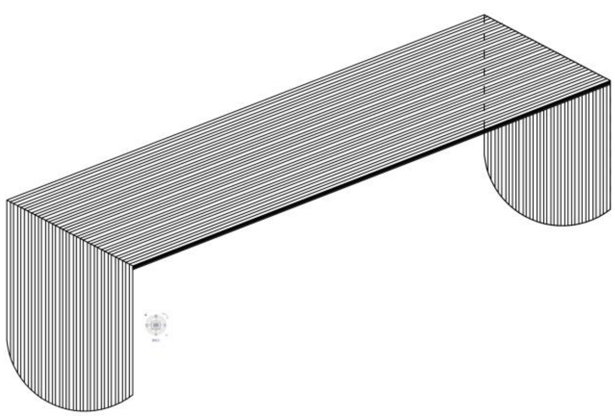

Also, the flat staple anchors are very competitive thanks to their low material cost of fabrication. The fig. represents the 3D view of a staple anchors with the fibers directions aligned as shown. The fig shows, instead, the detail of the staples' leg. The vertical length of the leg – measured with the ruler in the figure - represents the depth of the anchor, while the horizontal length – longitudinal to the position of the ruler in the figure – represents the width of the anchor.

Table 1.1 – Carbon fibers characteristics

Vf = 60%

TYPICAL PROPERTIES	SI	US
Tensile Strength	1,850 MPa	268 ksi
Tensile Modulus	130 GPa	18.9 msi
Compressive Strength	1,320 MPa	191 ksi
Compressive Modulus	125 GPa	18.1 msi
Interlaminer Shear Strength	70 MPa	10 ksi
Glass Translation Temperature (Tg,G”)	120°C	248°F

The table describes the carbon fibers’ characteristics, which the flat staple (but also the round staple) anchors are made of.

1.1.3 Round staple

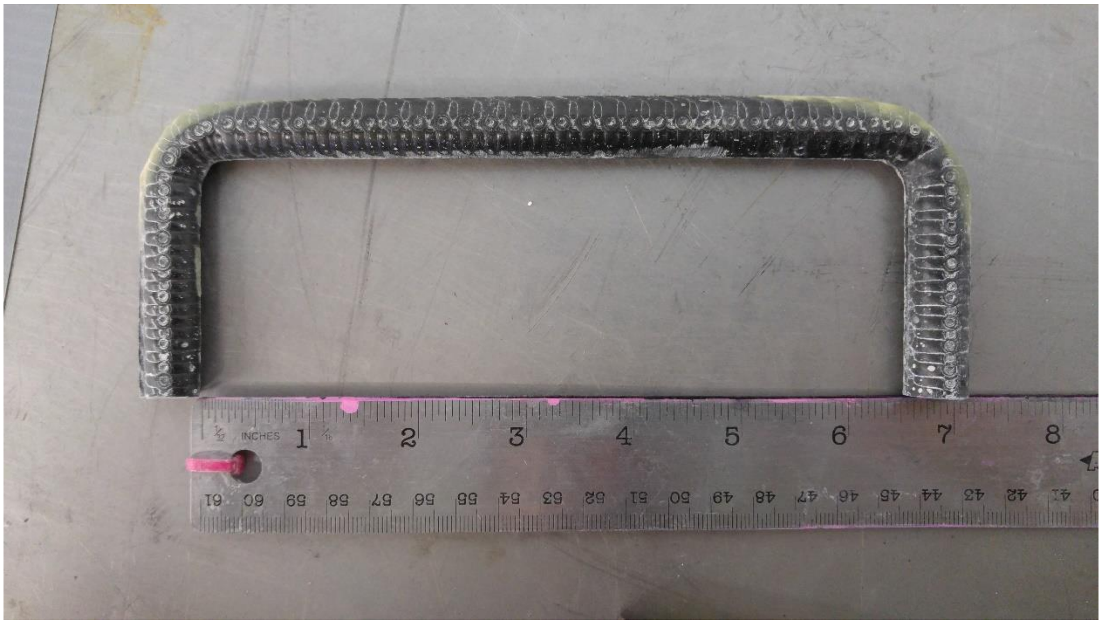

The round staple anchors are called so thanks to their rounded shape.

Again, the uni-directional fibers of the anchor are aligned in a longitudinal way to the flexural FRP sheet, covered by an epoxy layer that keeps the fibers together.

The following sketch represents the shape of a round staple anchor, without the indication of the fibers direction.

3D View

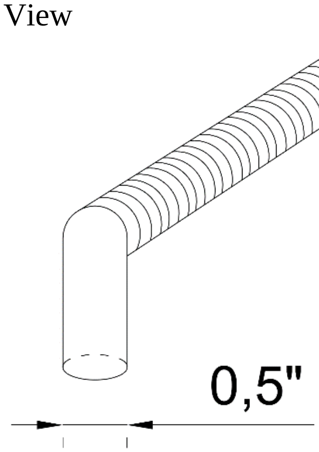

Cross-section

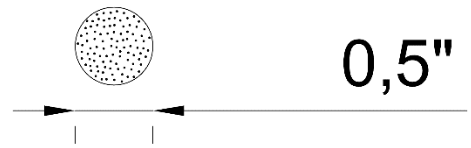

Cross-section

After a couple of specimens run with the round staple in the old shape configuration (sketch above), the round staples were improved. They were arranged in a new shape with 3 main important differences:

Firstly, the under part of the anchor is flat, increasing the area in contact with the FRP laminate

Secondly, the upper part of the anchor is no more rounded but elliptical, in order to prevent the formation of air bubbles in between the folded part of the flexural FRP sheet over the anchor and the anchor itself. Also, this shape allows the squeezed epoxy in excess to come out laterally, by the legs sides of the anchor.

Thirdly, many fibers were concentrated on the bend radius, improving the resistance in this location, where the stresses are more concentrated.

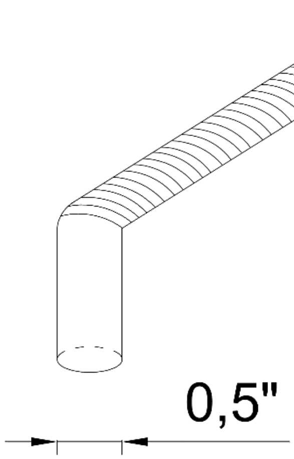

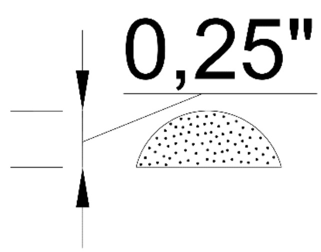

2. TEST RESULTS

The specimens were tested to examine the performance of the two types of anchors, the flat staple and the round staple anchors, in order to understand the improvements in terms of distribution of strains, stresses, peak loads and efficiencies given by installing a certain type of anchor. This chapter is divided into three main sections according to the main studies developed in this research.

The first section presents a full analysis of the results obtained from the flat staple anchorage system. Also, this section will compare the results given by a previous testing method used for the double shear test, in which the unbonded part of the CFRP wrapped around the steel support is dry.

The second section is dedicated to the results deduced from testing the round staple anchorage system. Here the test was conducted only with the new installation methodology (wet CFRP). In fact, after initial testing using the new installation (wet CFRP), this methodology revealed a significant success, which brought to test the following specimens (the round staples) only through this new installation.

The third section is a description of the failure modes observed in each single test.

2.1 FLAT STAPLES

As already described in the previous chapters, two different tests' series were run for the flat staples anchorage type.

2.1.1 Test 1 – Dry CRFP testing

The results from the test 1 refer to the results get from the dry CFRP configuration. In this first test 14 specimens were tested as:

- N° 2 benchmarks
- N° 3 3W_2D configuration (it states for 3 inches width and 2 inches depth)
- N° 3 3W_1D configuration
- N° 3 1,5W_2D configuration
- N° 3 1,5W_1D configuration

N.B: the W as capital letter means width, and the D as a capital letter refers to the depth of the anchor (in this way, for example, the "3W_2D configuration" it states for a 3 inches width and 2 inches depth anchor type. From now on, only this technical nomenclature will be used.

The following table (Table 2.6) summarizes the results in terms of peak loads, increases of the load (in percentage) with respect to the benchmark, rupture side, measured strains in the CFRP sheet and failure modes. The Peak Load P represents the maximum load applied by the hydraulic jack during the tests.

Shear test n.1 (DRY CFRP)

	Specimen ID	Anchor's dimensions	P [KN]	P/2 [KN]	Increase in Peak Load [%]	Rupture Side	Rupture Type	Strains in percentage at peak load SG1 [%]	SG2 [%]	SG3 [%]	SG4 [%]	SG5 [%]
BENCHMARKS	T1_BM_001	No anchor	45,80	22,90	34,53%		G	0,610	0,374	0,382	0,399	0,001
	T1_BM_002	No anchor	22,29	11,15	-34,53%		G					
		Average	34,05	17,02				0,610	0,374	0,382	0,399	0,001
		Standard deviation	11,76	5,88	**0,00%**			0,000	0,000	0,000	0,000	0,000
		C.V. [%]	34,53	34,53				0,000	0,000	0,000	0,000	0,000
FLAT STAPLES	T1_FS_3W_2D_001	3''W - 2''D	32,33	16,16	-5,06%	Left (instrumented side)	G	0,662	0,274	0,422	0,402	0,002
	T1_FS_3W_2D_002	3''W - 2''D	88,04	44,02	158,57%	Left (instrumented side)	G/C	1,007	0,722	0,684	0,670	0,006
	T1_FS_3W_2D_003	3''W - 2''D	61,16	30,58	79,62%	Left (instrumented side)	G					
		Average	60,51	30,25				0,835	0,498	0,553	0,536	0,004
		Standard deviation	22,75	11,37	**158,57%**							
		C.V. [%]	37,60	37,60								
	T1_FS_3W_1D_001	3''W - 1''D	67,11	33,56	97,11%	Left (instrumented side)	G	0,837	0,272	0,667	0,657	0,001
	T1_FS_3W_1D_002	3''W - 1''D	83,55	41,78	145,40%	Left (instrumented side)	G/C	0,815	0,498	0,464	0,170	0,003
	T1_FS_3W_1D_003	3''W - 1''D	67,31	33,65	97,68%	Right (not instrumented side)	G	0,815	0,373	0,620	0,448	0,000
		Average	72,66	36,33				0,823	0,381	0,584	0,425	0,001
		Standard deviation	7,71	3,85	**145,40%**							
		C.V. [%]	10,60	10,60								
	T1_FS_1,5W_2D_001	1,5''W - 2''D	61,60	30,80	80,91%	Right (not instrumented side)	G	0,782	0,206	0,320	0,605	0,003
	T1_FS_1,5W_2D_002	1,5''W - 2''D	34,25	17,12	0,59%	Left (instrumented side)	G					
	T1_FS_1,5W_2D_003	1,5''W - 2''D	86,35	43,18	153,62%	Left (instrumented side)	G/C	0,880	0,529	0,268	0,315	0,004
		Average	60,73	30,37				0,831	0,367	0,294	0,460	0,004
		Standard deviation	21,28	10,64	**153,62%**							
		C.V. [%]	35,04	35,04								
	T1_FS_1,5W_1D_001	1,5''W - 1''D	59,67	29,83	75,25%	Right (not instrumented side)	G	0,853	1,314	0,594	0,463	0,003
	T1_FS_1,5W_1D_002	1,5''W - 1''D	86,41	43,20	153,78%	Left (instrumented side)	G/C	0,788	0,513	0,377	0,893	0,014
	T1_FS_1,5W_1D_003	1,5''W - 1''D	64,89	32,44	90,57%	Right (not instrumented side)	G	1,014	0,6365	0,4983	0,6522	0,000
		Average	70,32	35,16				0,885	0,821	0,490	0,669	0,006
		Standard deviation	11,57	5,79	**153,78%**							
		C.V. [%]	16,46	16,46								

Table 2.1 – Summary test 1

It is very important to remind that, for all the tests run for this research, the side without strain gauges was strengthened with another FRP sheet over the anchor, covering in this way all the bonded area, in order to make each specimen fail on the other side provided with the instrumentation of the strain gauges. For this reason, in the table 2.1, there is also a column “rupture side” which explain if the rupture occurred on the expected left side (the instrumented one) or on the reinforced side (on the right side, the one not instrumented). From this table, we can also easily understand that most of the test were useless. That is because the rupture did not occur on the bonded part, where the anchor was installed, but on the dry CFRP, outside the bond area at a relatively low-stress level compared with the tensile strength of the CFRP itself. This might be caused by four main reasons:

- Different stresses distribution on the dry CFRP, caused by the not perfectly centered applied load, that brought to a rip in the most stressed fiber, causing the cracking start. It is important to remind that in the dry CFRP, as soon as a little crack occur, this immediately propagate toward the closest dry fibers, leading to the crack of the entire CFRP sheet.
- The unevenness of adhesive on CFRP sheet out of the bond area, leading to uneven stress distribution in the CFRP fibers.
- The application of the epoxy resin on CFRP sheet out of the bond area, leading again to uneven stress distribution in the CFRP fibers.
- The low unbounded area furnished on the concrete surface (only 1 inch), which could have caused again an uneven stress distribution in the CFRP fibers, just out of the bonded area where most of the ruptures occurred.

For all these reasons, the results of this first test are overall senseless. Only 4 specimens highlighted in green (table 2.1) failed as soon as the debonding initiated. Unfortunately, even if a correlation between different depths could have been obtained from those 4 specimens, that would not make any sense because of the very low peak load they reached if compared to the successful test 2. Also, by read the strains, we can easily understand why the strain gauge number 1 was the most stressed since this is the strain located exactly where the rupture occurred. In this way, we will not get in the depth of this first test, but we will analyze the results of the second test, in which, thanks to the new installation provided, all the specimens succeeded, providing reasonable results and very interesting data analysis.

2.1.2 Test 2 – Wet CRFP testing

The results from the test 2 refer to the results obtained from the dry CFRP installing method. In this second and successful test, 12 specimens were tested as it follows:

- N° 3 benchmarks
- N° 3 3W_1D configuration (it states for 3 inches width and 2 inches depth)
- N° 3 2W_1D configuration
- N° 3 1W_1D configuration

Table 2.2 – Summary test 2 -– Flat staples

Shear test n.2 (WET FRP)

	Specimen ID	Anchor's dimensions	P/2 [KN]	Increase in Peak Load [%]	Rupture Side	Rupture Type	Strains in % at peak load					Increase in % of strains at the peak load				
							SG1 [%]	SG2 [%]	SG3 [%]	SG4 [%]	SG5 [%]	SG1 [%]	SG2 [%]	SG3 [%]	SG4 [%]	SG5 [%]
BENCHMARKS	T2_BM_001	No anchor	29,01	-19,68%	Left (instrum.side)	A	0,340	0,276	0,302	0,530	0,021	0,00%	-18,61%	-22,86%	9,16%	59,99%
	T2_BM_002	No anchor	37,88	4,91%	Right (not instrum. side)	A	x	0,402	0,482	0,441	0,005	x	18,61%	22,86%	-9,16%	-59,99%
	T2_BM_003	No anchor	41,45	14,77%	Right(not instrum. side)	A	x	x	x	x	x	x	x	x	x	x
		Average	36,11				0,340	0,339	0,392	0,485	0,013	0,00%	0,00%	0,00%	0,00%	0,00%
		Standard deviation	4,44	**0,00%**			0,000	0,063	0,090	0,044	0,008					
		C.V. [%]	12,29				0,000	0,186	22,863	9,164	59,988					
FLAT STAPLES	T2_FS_3W_001	3''W - 1''D	55,37	53,34%	Left (instrum. side)	C	0,196	0,134	0,524	1,298	0,411	-42,33%	-60,32%	33,61%	167,54%	3015,60%
	T2_FS_3W_002	3''W - 1''D	62,26	72,41%	Left (instrum. side)	F	0,459	0,148	0,481	0,729	0,038	34,93%	-56,43%	22,71%	50,25%	190,41%
	T2_FS_3W_003	3''W - 1''D	81,62	126,01%	Right (not instrum. side)	F	0,414	0,197	x	0,374	x	21,47%	-41,80%	x	-22,94%	x
		Average	66,42				0,356	0,160	0,502	0,800	0,225	4,69%	-52,85%	28,16%	64,95%	1603,00%
		Standard deviation	11,11	**83,92%**												
		C.V. [%]	16,73													
	T2_FS_2W_001	2''W - 1''D	54,78	51,69%	Left (instrum. side)	B	0,293	0,878	0,654	0,584	0,082	-14,04%	159,47%	66,88%	20,30%	524,79%
	T2_FS_2W_002	2''W - 1''D	66,98	85,49%	Left (instrum. side)	C/F	0,245	0,379	0,677	0,559	x	-27,97%	11,96%	72,65%	15,23%	x
	T2_FS_2W_003	2''W - 1''D	64,88	79,65%	Left (instrum. side)	C/F	x	x	x	x	x	x	x	x	x	x
		Average	62,21				0,269	0,629	0,665	0,571	0,082	-21,00%	85,72%	69,76%	17,76%	524,79%
		Standard deviation	5,33	**72,28%**												
		C.V. [%]	8,56													
	T2_FS_1W_001	1''W - 1''D	57,18	58,34%	Left (instrum. side)	C	0,115	0,513	0,399	0,405	0,049	-66,36%	51,64%	1,74%	-16,46%	268,50%
	T2_FS_1W_002	1''W - 1''D	55,69	54,21%	Left (instrum.side)	C	0,331	0,204	0,545	0,966	x	-2,79%	-39,85%	39,04%	99,24%	x
	T2_FS_1W_003	1''W - 1''D	59,17	63,84%	Left (instrum.side)	C	x	x	x	x	x	x	x	x	x	x
		Average	57,35				0,223	0,358	0,472	0,686	0,049	-34,58%	5,89%	20,39%	41,39%	268,50%
		Standard deviation	1,42	**58,80%**												
		C.V. [%]	2,48													

As shown in the table above (Table 2.2), the average peak load gradually increased from the specimens without anchors (T2_BM) to the specimens with anchors, depending on the type of anchor installed and the configuration adopted. While characterizing the anchor resistance in terms of load, we must refer to the load identified as $\frac{P}{2}$ because this represents the load applied to one side.

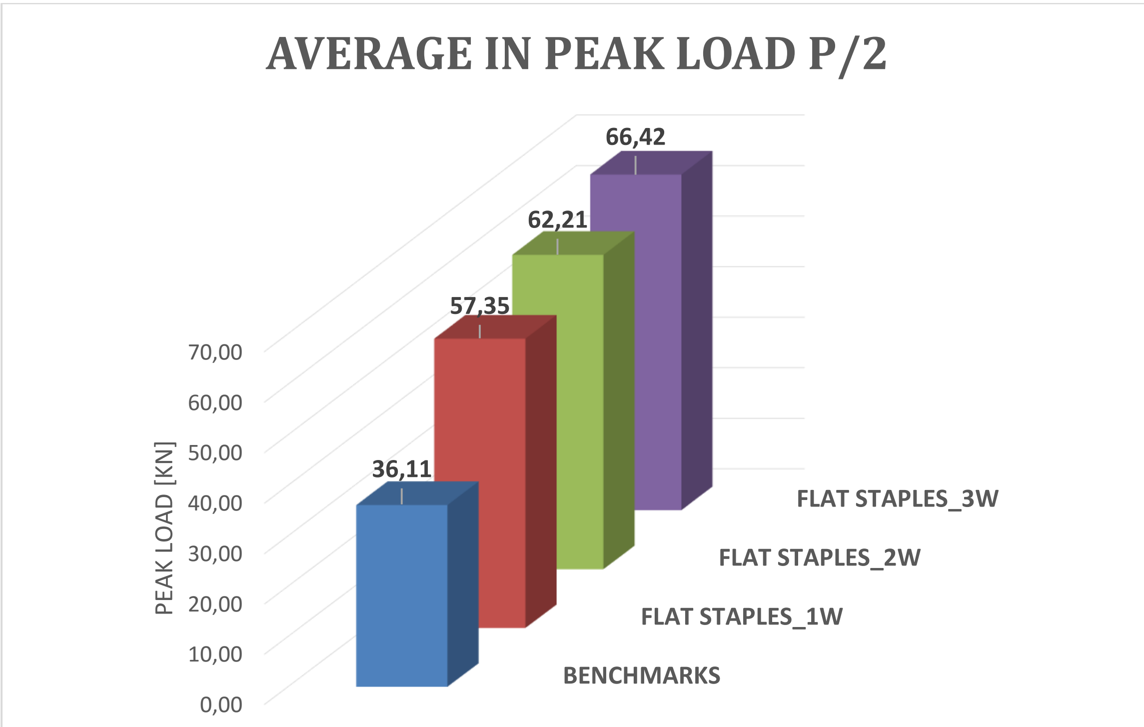

Figure 2.1 – Peak loads' average of all the specimens

The previous Fig. 2.1 represents the average in terms of peak loads reached by the specimens.

Herein it is interesting here to compare the theoretical peak load calculated (thanks to the CNR formulas) which is 38,53 KN, with the average of the peak load obtained from the experimental results, which is 36,11 KN. This good correspondence between the theoretical peak load and the real peak load is crucial to give reliability to the results obtained from the test 2.

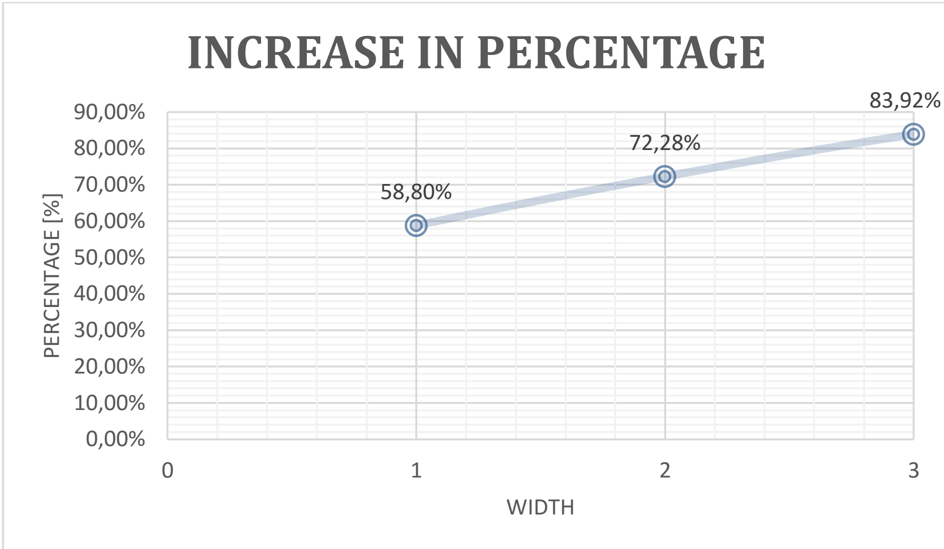

Figure 2.2 – Increase in percentage of the peak loads' average of all the specimens

In Fig. 2.2 is shown the increase in percentage reached by the average of the types of anchor system installed. It is interesting to notice that the increase it is not linear, but logarithmic. This is an important fact that should be considered while choosing the best configuration, as it will be explained in the appropriate chapter 3.2.

<u>*2.1.2.1 Strain gauges readings*</u>

Benchmarks

A typical strain distribution along the bonded length of the CFRP material is shown in fig. 2.3 and 2.4

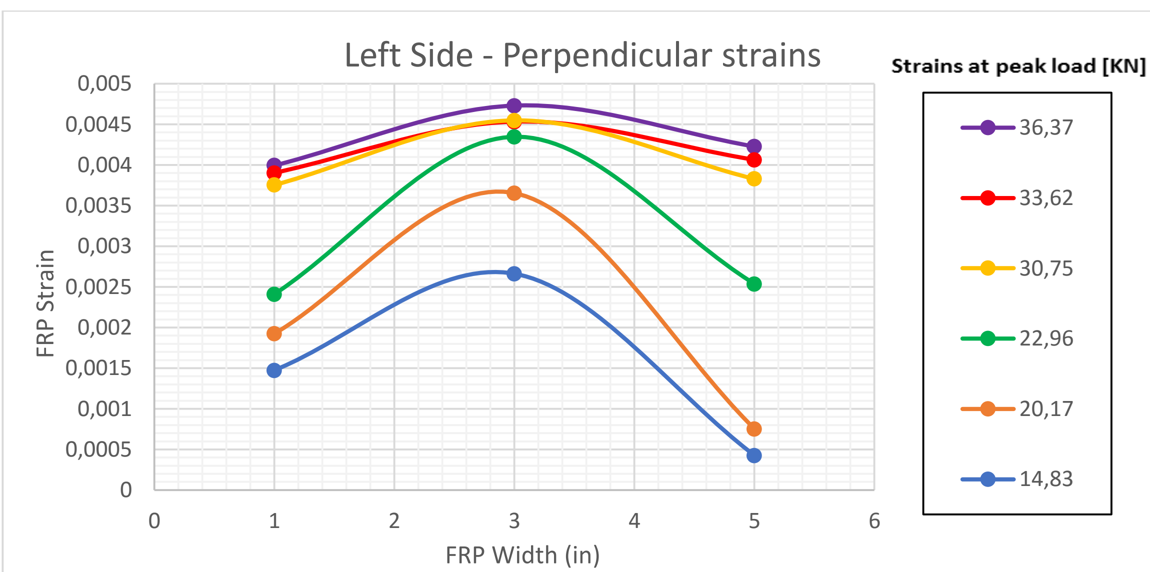

Figure 2.3 – Perpendicular strain distribution of a benchmark

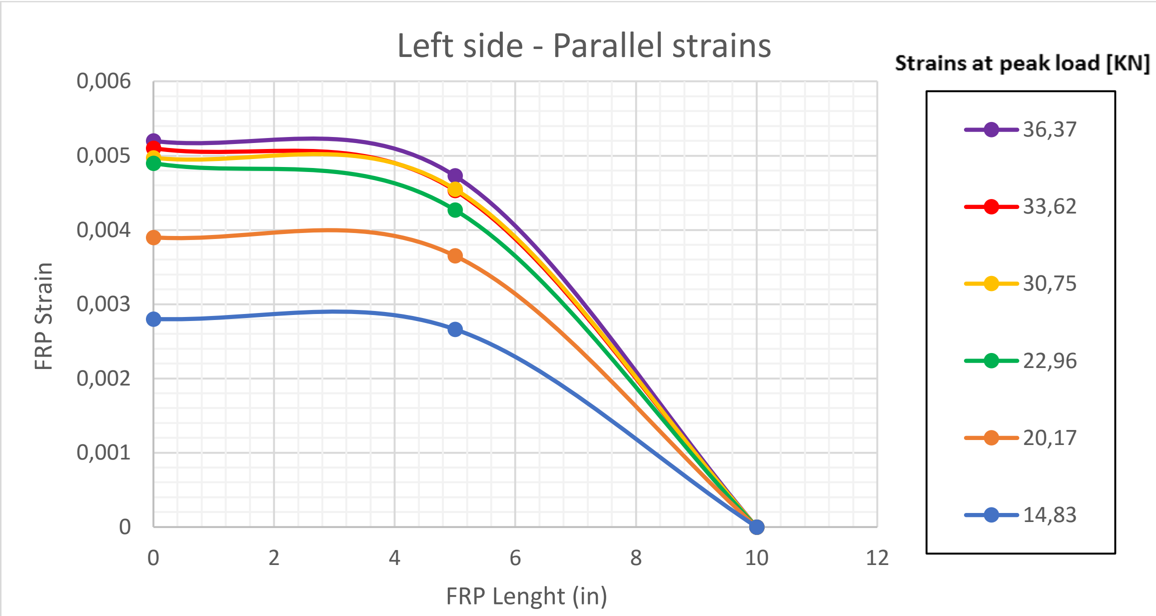

Figure 2.4 - Parallel strain distribution of a benchmark

The Fig. 2.3 and Fig. 2.4 above refer to a benchmark sample, the one with no anchor installed.

The Fig. 2.3 shows the trend of the perpendicular strain, the ones longitudinal to the CFRP fibers' axis.

In particular, the x-axis represents the width of the CFRP sheet in inches. In this way, all the points settled at 1 inch identify the readings from the S.G. 2, all the points settled at 3 inches are the readings taken from the S.G. 3 and the points on the 5th inch represent the readings taken from the S.G. 4.

The following Fig. 2.5 illustrates the location of the strain gauges, with the relative distance between all of them.

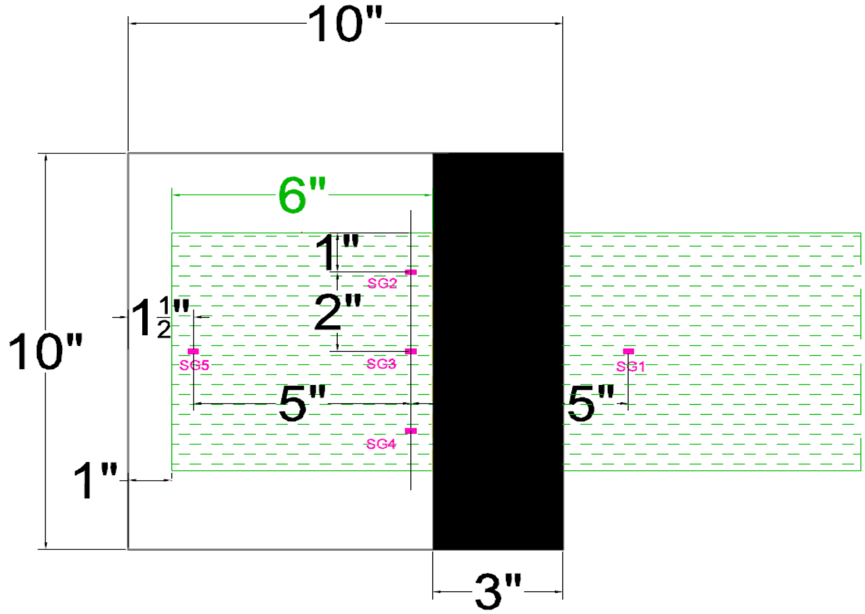

Figure 2.5 - Strain gauges position

Again, from the reading of the strain gauges in the Fig. 2.3, it is interesting to notice how for this benchmark the applied load was well distributed along the entire length of the CFRP sheet. Indeed, the ending curves (30,75 KN, 33,62 KN and 36,37 KN) assume a flat trend, while the SG.2 and S.G. 4 read more or less the same strains' value.

That typical trend is mean of a good and well-distributed applied load (from the hydraulic jack) all along the 6" width of the CFRP.

The Fig. 2.4, instead, represents the strains' distribution on the fibers' axis, and the points along the 0 inch width represent the S.G. 1, while the points on the 5th inch are the readings from the S.G. 3, and finally the readings at the 10th inch are the ones registered by the S.G. 5. Here, it is interesting to underline how the strains' read by the S.G. 1 and are a little more high from the ones' read by the S.G. 3. This is most due to the fact that, since no anchor where installed in this sample, the progressive behavior of the debonding crack initiated from the loaded end (readings of the S.G. 1) with high strains' values, propagating all through the bonded length to the points where the strain diminishes significantly, at the free ends.

FLAT STAPLE 2W_1D_001

Below, the strains' results of the flat staple 2W_1D_001 are shown.

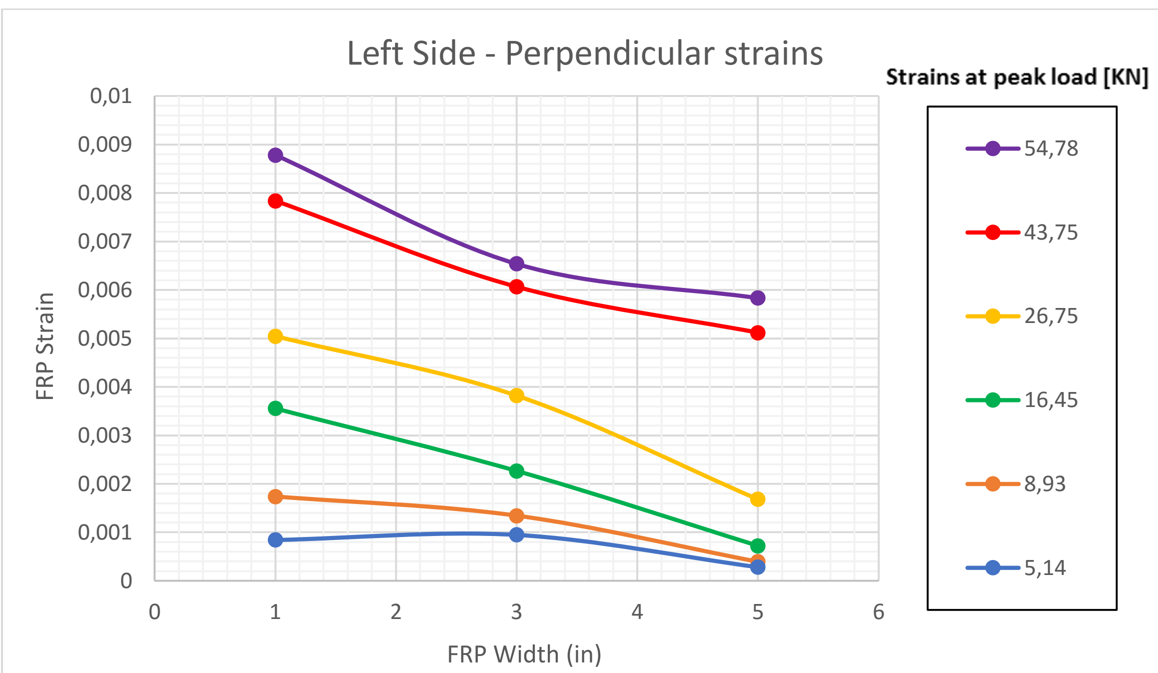

Figure 2.6 - Perpendicular strain distribution of the T2_FS_2W_1D_001

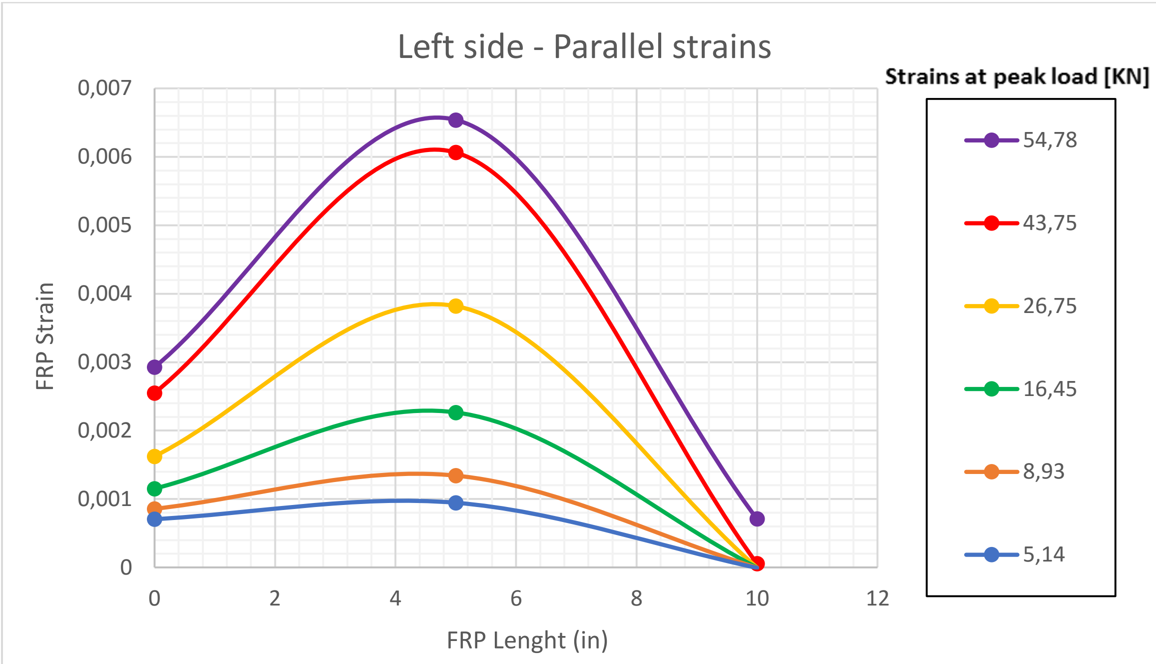

Figure 2.7 - Parallel strain distribution of the T2_FS_2W_1D_001

From these two images, it is possible to notice two main differences between the benchmark.

- Firstly, the strain gauges S.G. 2, 3 and 4 recorded higher values than the ones read from the benchmark. The S.G. 2, 3 and 4 are considered the most important, due to the fact that are placed in the in front of the anchor. This region is of particular interest being the sheet fibers directly engaged by the anchor. The recorded values are the greatest ones in terms of deformation and they may be considered as the bond capacity of the system.

- Secondly, the Fig. 1.7 clearly shows how the S.G. 3 read an higher value compared to the S.G. 1, contrarily from what the benchmark displayed. Again, this is a proof of the effective anchor work

- Thirdly, as the crack system occurred, the S.G. 5, recorded a sudden alteration, leaping immediately to high values of strain. Here is shown only the strain recorded at the very peak load, but after that, it is important to say that the value increased by 1%. This fact has been noticed in every specimen that was provided with an anchor system.

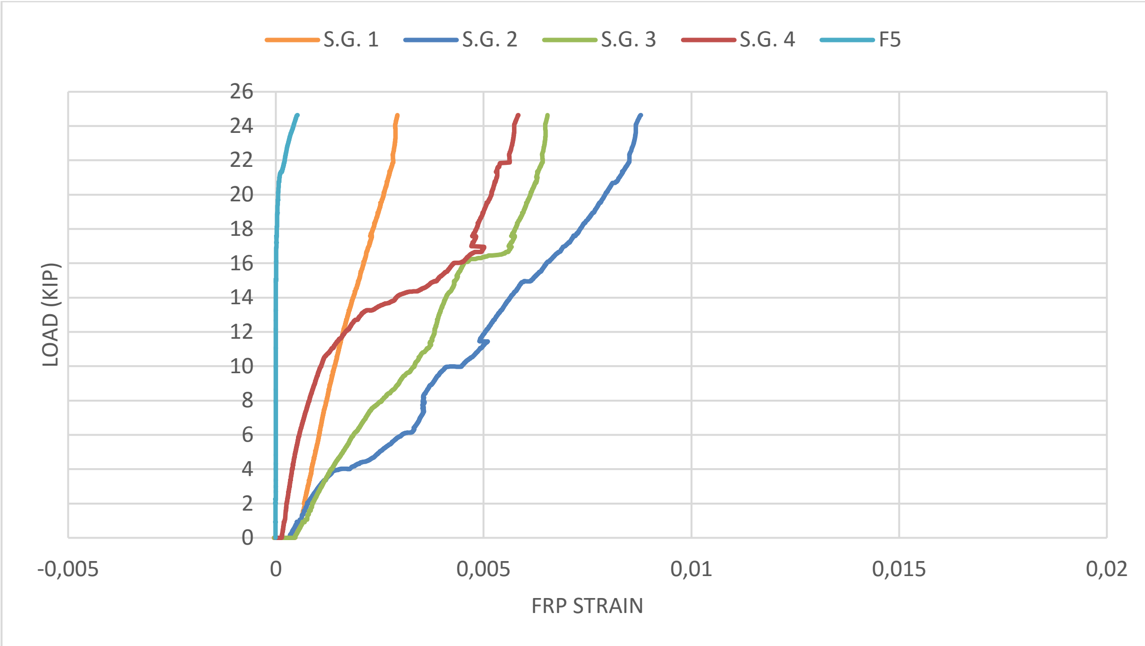

Figure 2.8 – Load - strain curve of the T2_FS_2W_1D_001

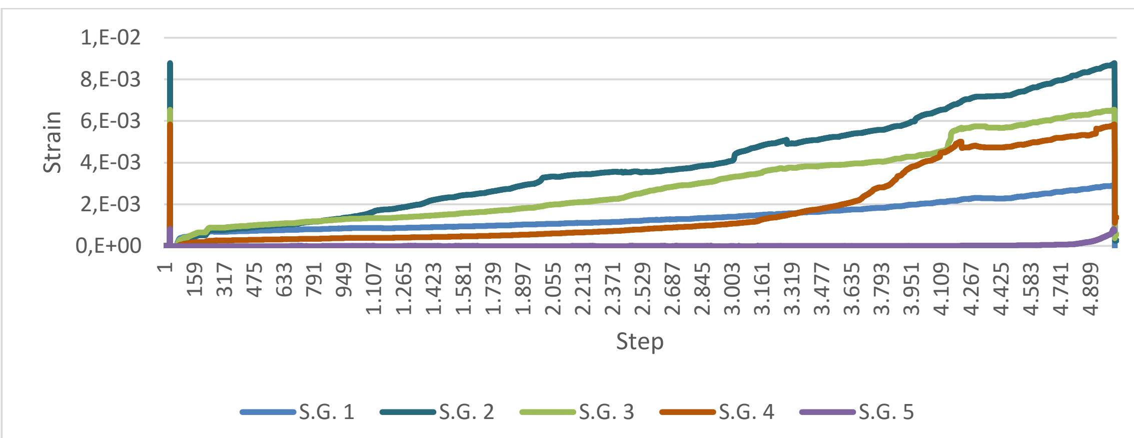

Figure 2.9 – Load - time curve of the T2_FS_2W_1D_001

The strain readings taken at different locations along the bond length (S.G. 2, S.G.3, S.G.4, S.G.5) and the unbonded length (S.G.1) show the progressive behavior of the debonding crack, which initiated at the loaded end (readings of the S.G. 2, S.G.3, S.G.4) and propagated towards the free end, behind the anchor as the reading of the S.G. 5. The fig 1.8 wants to show how, as the interfacial crack propagates through the monitored locations, it is evident the sudden change in the stiffness of the load, identified with a change in the trend of the stress-strain curve of the affected strain gauges. The Fig. 2.9 shows instead the variation of the strain/time. In that figure, the numbers identify ad step represents the rows of the data read by the DAQ (data acquisition system).

FLAT STAPLE 3W_1D_002

Below, the strains' results of the flat staple 3W_1D_002 are shown.

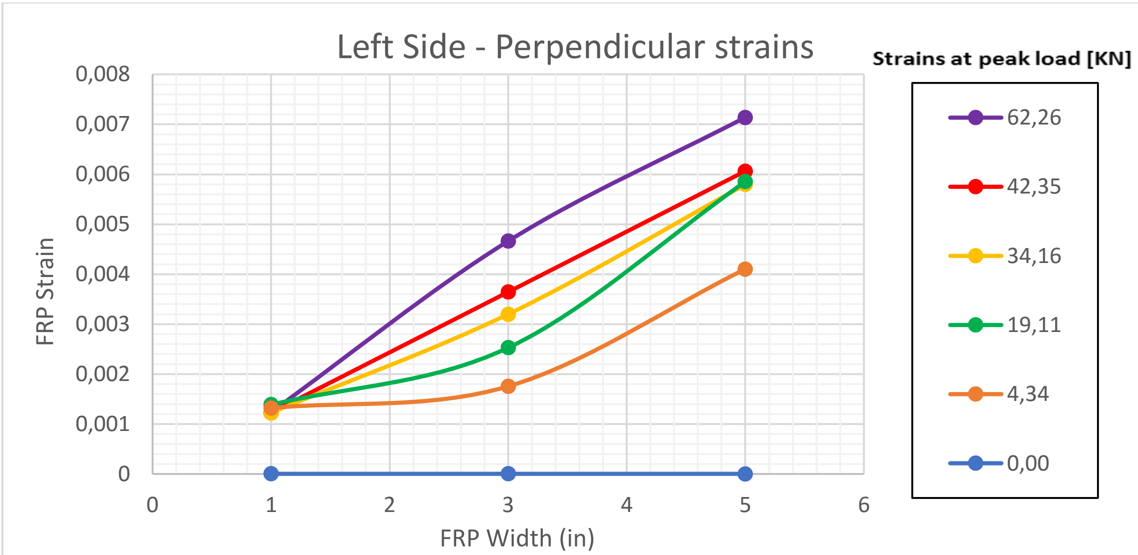

Figure 2.10 – Perpendicular strain distribution of the T2_FS_3W_1D_002

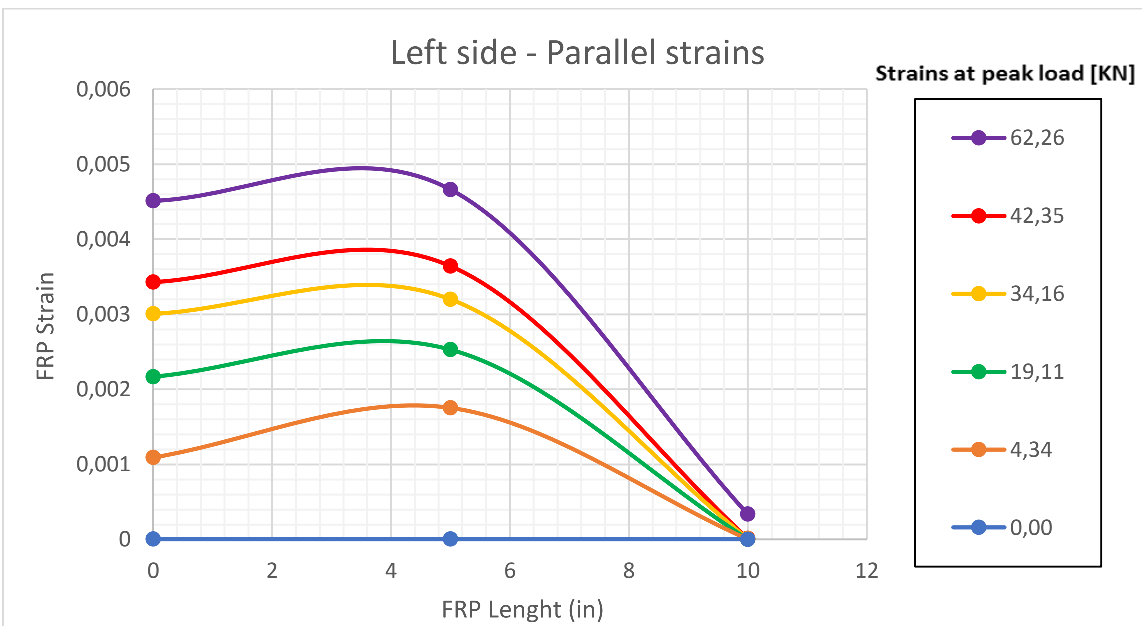

Figure 2.11 – Parallel strain distribution of the T2_FS_3W_1D_002

This case it is introduced to underline an important fact that was observed.

From the readings of S.G. 2, 3 and 4 in Fig. 2.11, it is clearly possible to see that the strains are very bad-distributed. In fact, an important aspect of the double shear test that has to be underlined is related with its set up: the results obtained from the tests were found to be highly dependent on the alignment of the system. Perfect alignment was very difficult to ensure and different degrees of load eccentricity were observed. Moreover, the specimens were found to be very sensitive to the handling operations. This has to be noticed especially from the first test run. With the test 2, even if the load was not completely centered and the system not perfectly aligned, this problematic seems to have been overcome.

Here it is proposed the same case but with the old installation, from the test n.1:

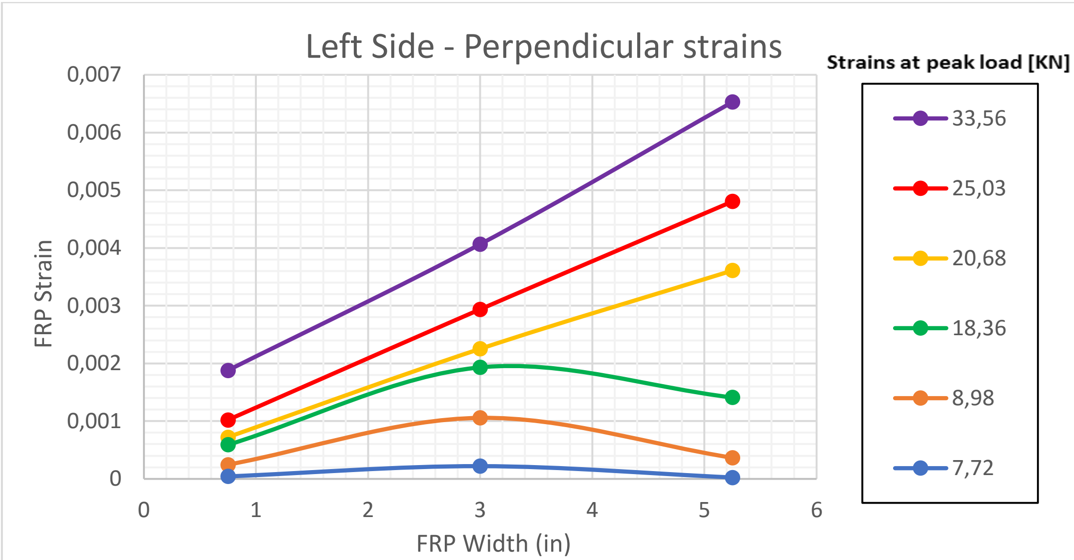

Figure 2.12 – Perpendicular strain distribution of the T1_FS_3W_1D_001

Immediately, we notice how the different distribution of strains made the system's collapse for the test n.1, while the test n. 2, even the bad distribution of strains, was successful. This reason is due to the fact that the new installation provides the entire CFRP sheets acting as a matrix. The Graph in fig. 2.12 refers to the specimen T1_FS_3W_1D_001 (referred to the test's results in table 1.1).

FLAT STAPLE 1W_1D_001

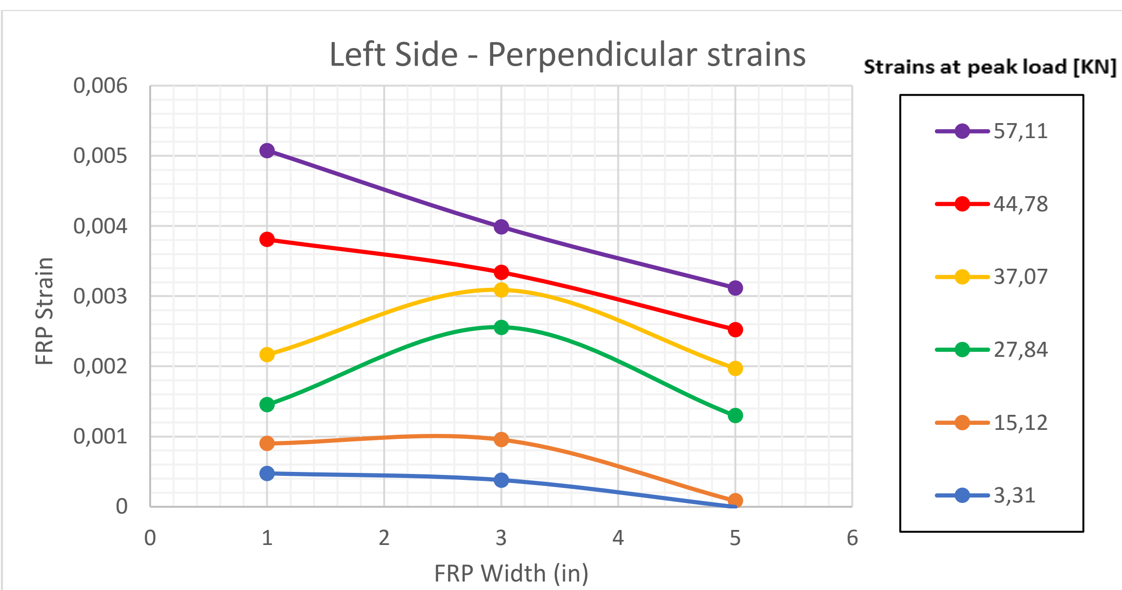

Figure 2.13 – Perpendicular strain distribution of the T2_FS_1W_1D_001

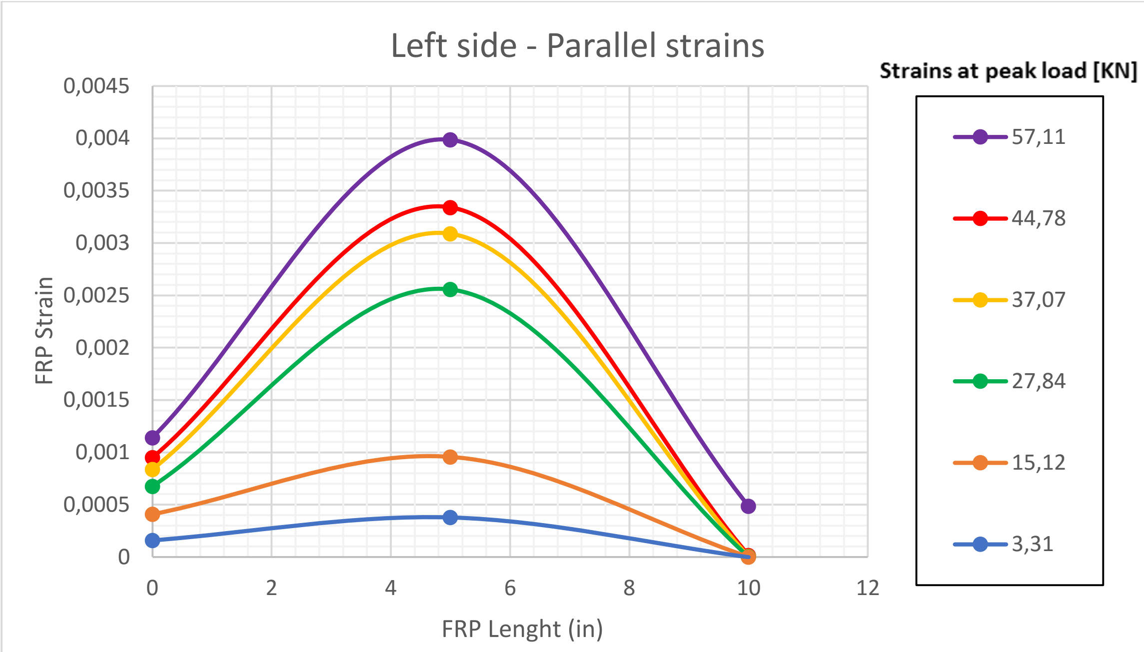

Figure 2.14 – Parallel strain distribution of the T2_FS_1W_1D_001

Below, in fig. 2.15 the graphs referred to the average's readings of strain gauges n.1 and n.3 are plotted.

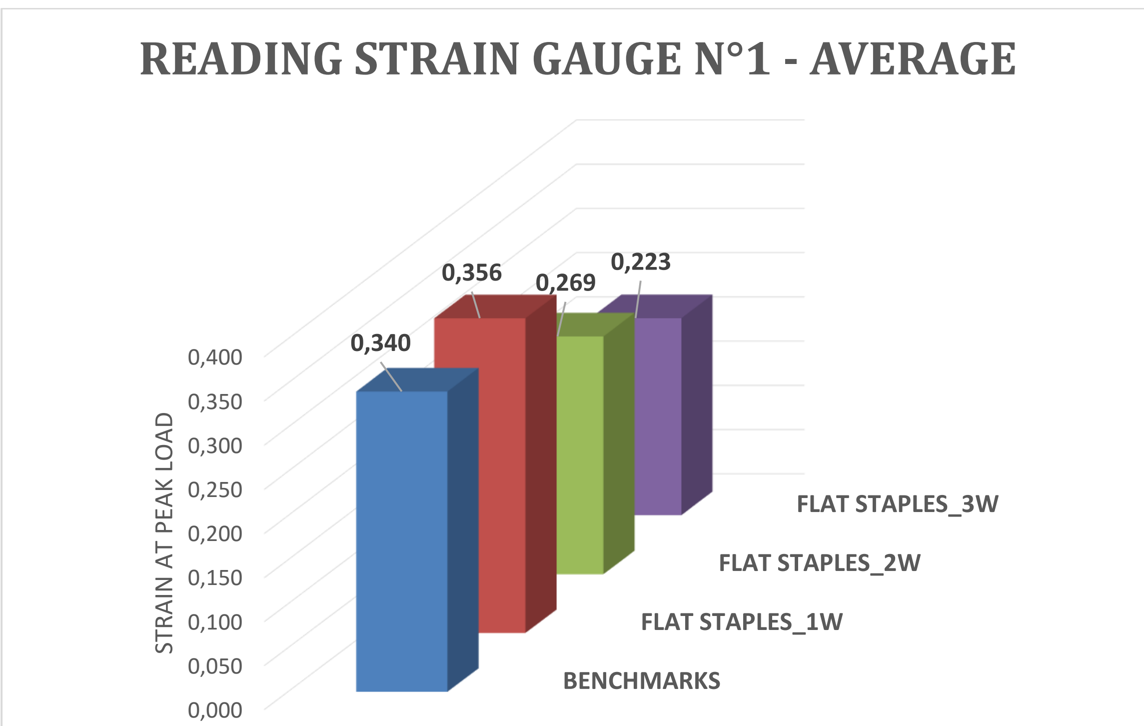

Figure 2.15 – Average values of the strain gauges n°1

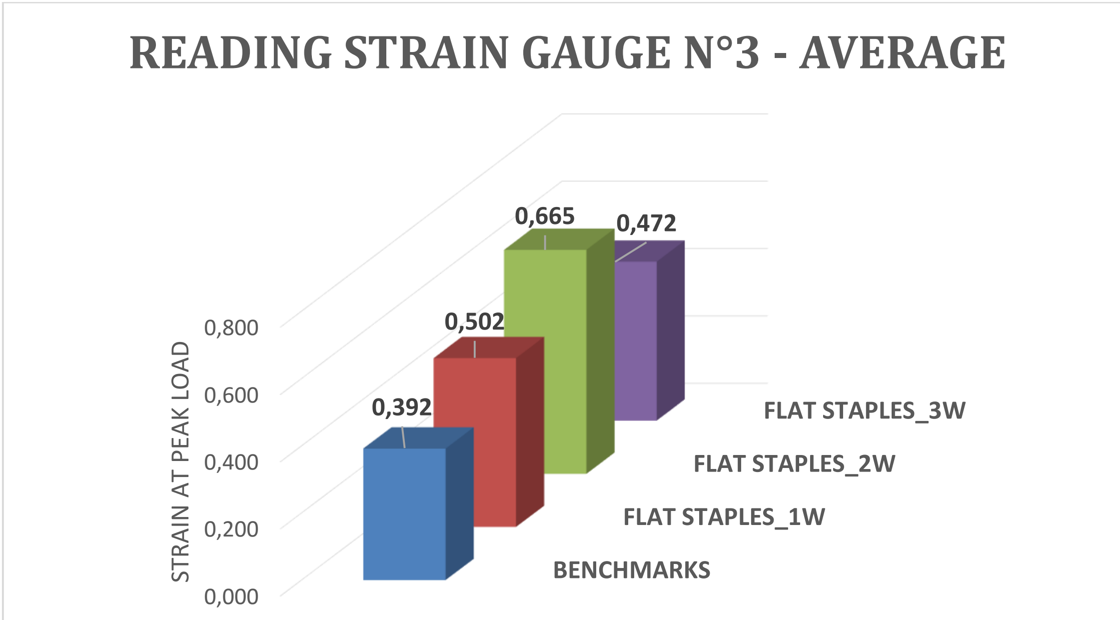

Figure 2.16 – Average values of the strain gauges n°3

Again, there is consistency between al the results deducted and all the claims previously made are here collected in terms of average between all the samples run.

2.2 ROUND STAPLES

2.2.1 Test 2 – Wet CRFP testing

The round staples anchors were run with the wet CFRP installation. 9 more specimens here were tested as:

- N° 3 RS_2D configuration (it states for 3 inches width and 2 inches depth)
- N° 3 RS_1D configuration
- N° 3 DRS_1D configuration

The same benchmarks, which were run for the characterization of the flat staple anchors, were used.

N.B: the RS as capital letters means Round Staple, DRS means Double Round Staple and the D as a capital letter refers to the depth of the anchor (in this way, for example, the "DRS_1D configuration" it states for a 1-inch depth in double round staple configuration. From now on, only this technical nomenclature will be used.

Again, the following table summarizes the results in terms of peak loads, increases of the load and strains with respect to the benchmark, rupture side, measured strain in the FRP sheets and failure modes. Also, In this table, the first two results, which are referred to the 2-depth round staple configuration, has been crossed, since they were just a first prototype of the round staples anchors, while tests from the third one on are the experimental anchors in the new improved form.

Table 2.3 – Summary test 2 – Round staples

Shear test n.2 (WET FRP)																
	Specimen ID	Anchor's dimensions	P/2 [KN]	Increase in Peak Load [%]	Rupture Side	Rupture Type	Strains in % at peak load					Increase in % of strains at the peak load				
							SG1 [%]	SG2 [%]	SG3 [%]	SG4 [%]	SG5 [%]	SG1 [%]	SG2 [%]	SG3 [%]	SG4 [%]	SG5 [%]
ROUND STAPLES	RS_2D_001	2''D_OLD	30,75	-14,86%	Left (instrum. side)	D	0,241	0,317	0,517	0,600	0,013	-29,11%	-6,44%	31,95%	23,64%	-2,95%
	RS_2D_002	2''D_OLD	36,49	1,05%	Left (instrum. side)	C/D	0,339	0,223	0,070	0,064	0,550	-0,50%	-34,00%	-82,04%	-86,78%	4067,28%
	RS_2D_003	2''D_NEW	49,13	36,06%	Left (instrum. side)	D	0,104	x	0,191	0,304	x	-69,39%	x	-51,37%	-37,28%	x
		Average	49,13				0,228	0,270	0,259	0,323	0,281	-33,00%	-20,22%	-33,82%	-33,48%	2032,17%
		Standard deviation	0,00	**36,06%**												
		C.V. [%]	0,00													
	RS_1D_001	1''D_NEW	46,34	28,31%	Right (not instrum. side)	E	0,218	0,140	0,295	0,120	x	-36,05%	-58,58%	-24,85%	-75,24%	x
	RS_1D_002	1''D_NEW	59,20	63,94%	Left (instrum. side)	E	0,242	0,089	x	0,081	x	-28,82%	-73,62%	x	-83,40%	x
	RS_1D_003	1''D_NEW	52,31	44,86%	Right (not instrum. side)	D	0,333	0,085	0,219	0,397	x	-2,20%	-74,80%	-44,19%	-18,07%	x
		Average	52,62				0,264	0,105	0,257	0,199	x	-22,36%	-69,00%	-34,52%	-58,90%	x
		Standard deviation	5,26	**45,70%**												
		C.V. [%]	9,99													
	DRS_1D_001	1''D_NEW	65,13	80,35%	Left (instrum. side)	C	0,519	x	0,178	x	0,085	52,44%	x	-54,53%	x	544,50%
	DRS_1D_002	1''D_NEW	68,88	90,73%	Left (instrum. side)	C/F	0,376	x	0,258	x	0,065	10,37%	x	-34,29%	x	395,89%
	DRS_1D_003	1''D_NEW	62,84	74,02%	Left (instrum. side)	E	x	x	x	x	x		x		x	
		Average	65,61				0,447	x	0,218	x	0,075	31,40%	x	-44,41%	x	470,20%
		Standard deviation	2,49	**81,70%**												
		C.V. [%]	3,79													

ROUND STAPLE 2D_001

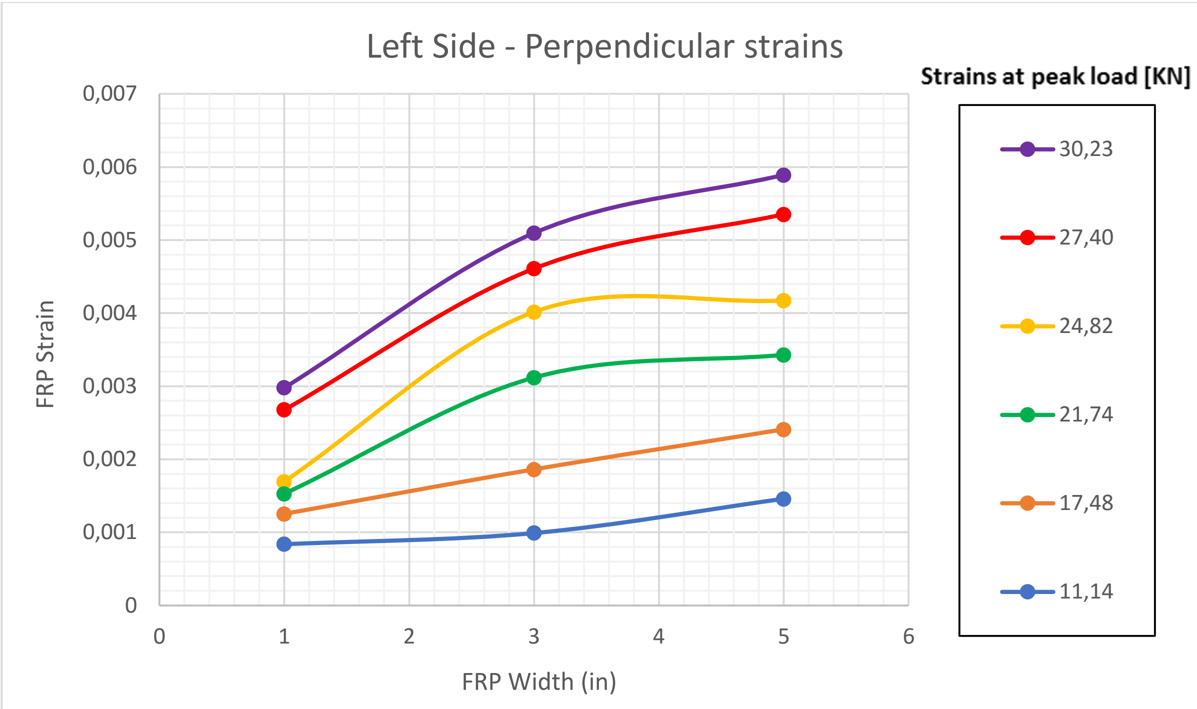

Figure 2.17 – Perpendicular strain distribution of the T2_RS_2D_001

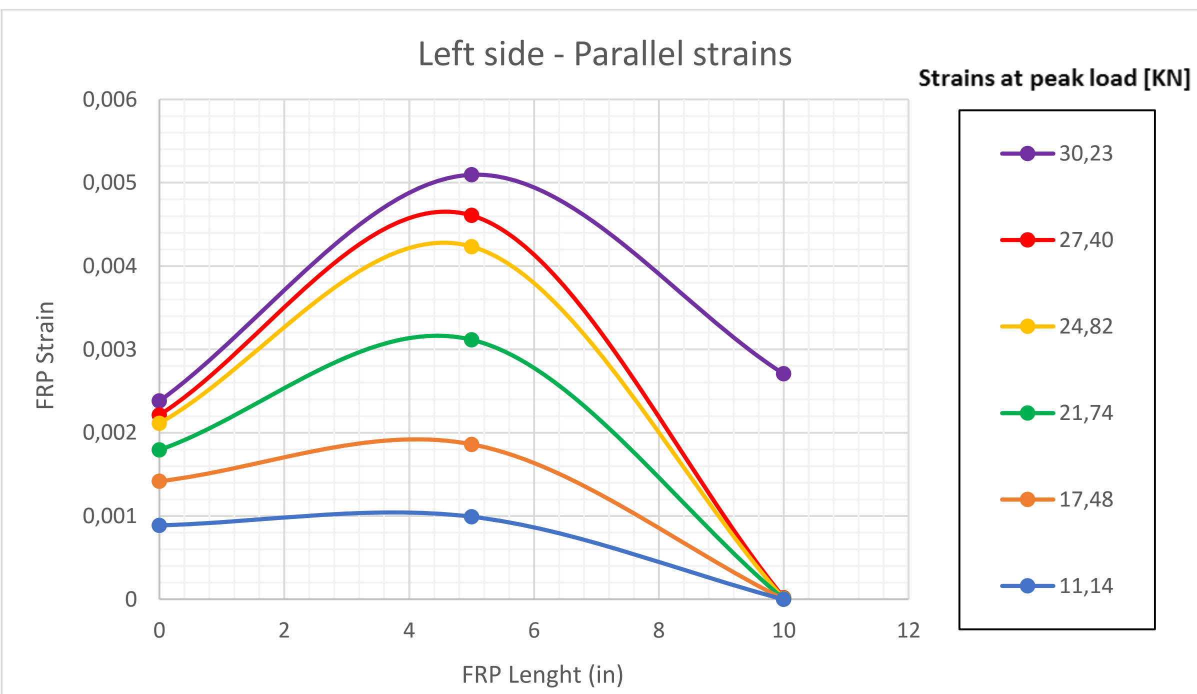

Figure 2.18 – Parallel strain distribution of the T2_RS_2D_001

For this specimen, it is important to underline that the S.G.2, 3 and 4, were positioned on the flexural sheet below the anchor. In fact, these strains show the same trend and behavior of to the ones installed on the flat staple anchors (previously shown in fig. 2.6, 2.7).

ROUND STAPLE 1D_001

The following Fig. 2.19 represents the strains' reading of the RS_1D_001. In this case, the S.G.2, 3 and 4 were installed on the flexural sheet above the anchor, in the wrapped part around the anchor that it covers entirely the latter.

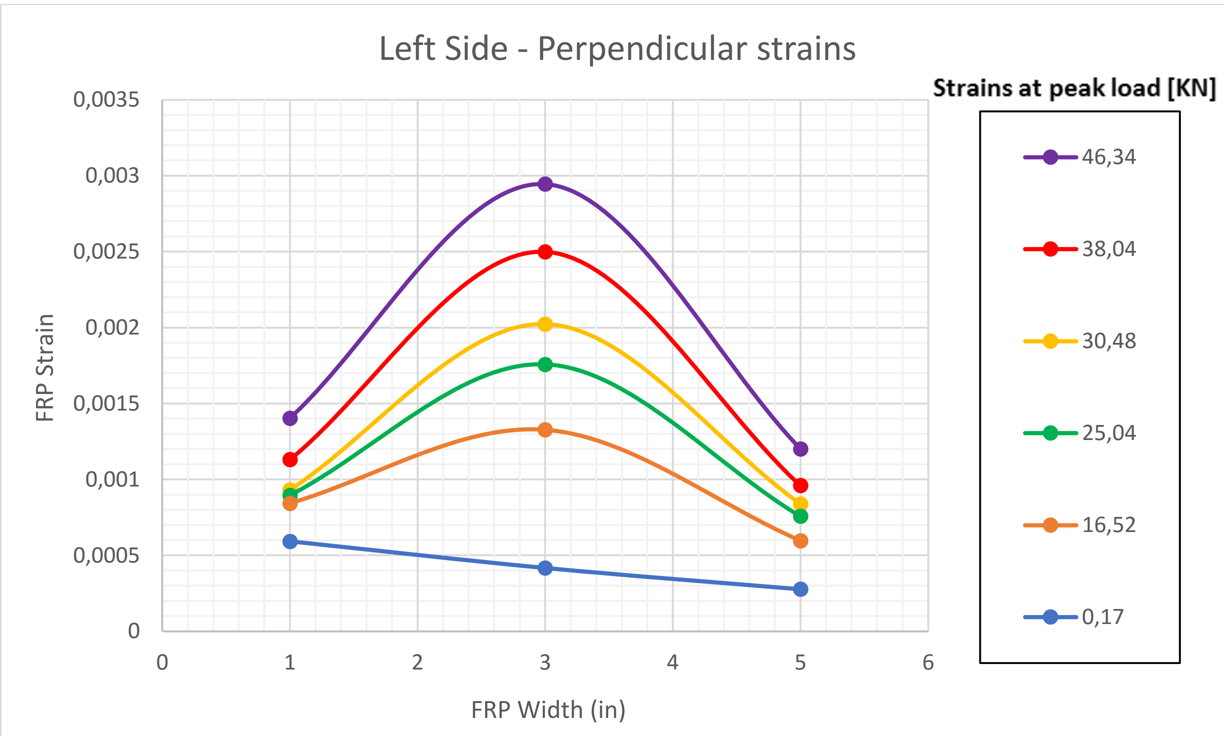

Figure 2.19 – Perpendicular strain distribution of the T2_RS_1D_001

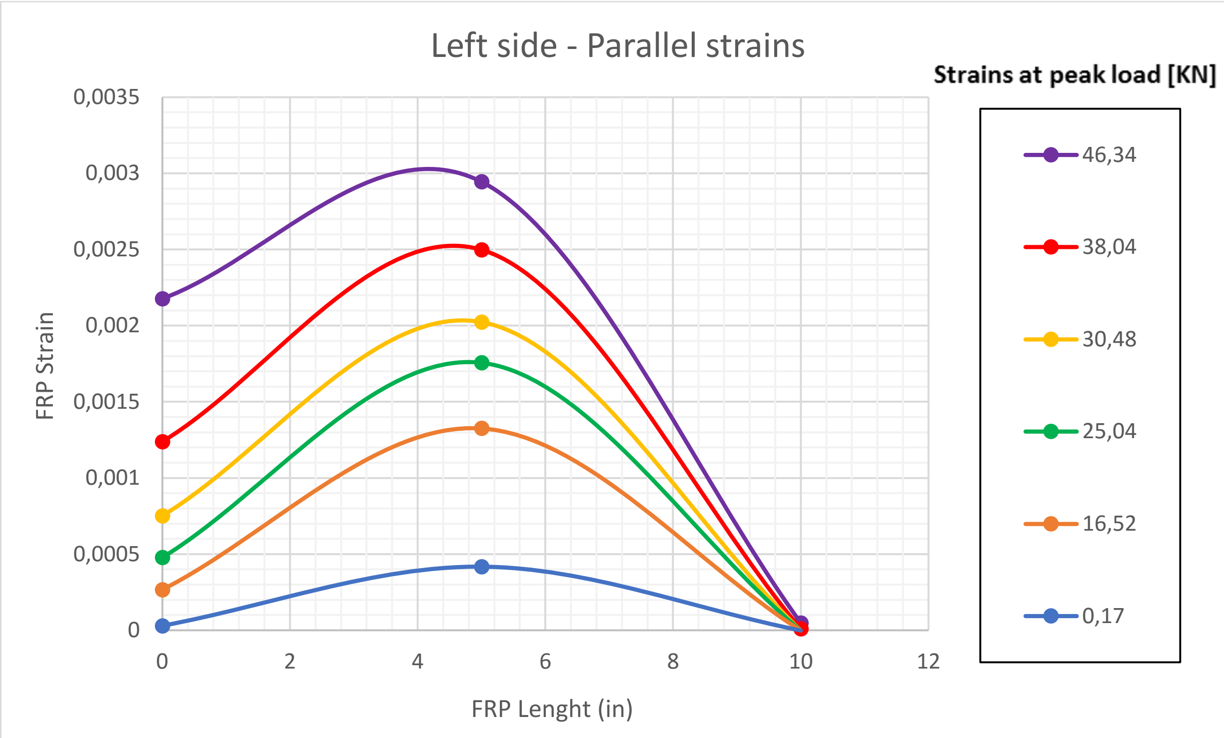

Figure 2.20 – Parallel strain distribution of the T2_RS_1D_001

In this case, it is interesting to notice how, in general, the trend is always the same, but the strains are much smaller as compared to the previous ones. In fact, the strain peak here is at 0,3%, while usually, it reaches values around 0,7 - 0,8%. This is because we double the nominal cross-sectional area from 152,4 mm^2 to 304,8 mm^2 . In fact, increasing the cross-sectional area of the CFRP, the strains decrease as the following formula:

$$\frac{Force}{E \cdot A} = \varepsilon$$

Where the Force (peak load) and the modulus of elasticity E remain constant.

It is important to underline how the 2-inches depth configuration does not produce any good improvement if related to the 1-inch depth. Also, as explained better in the Chapter 3, it has been stated that 1-inch depth is the best configuration (concrete cover).

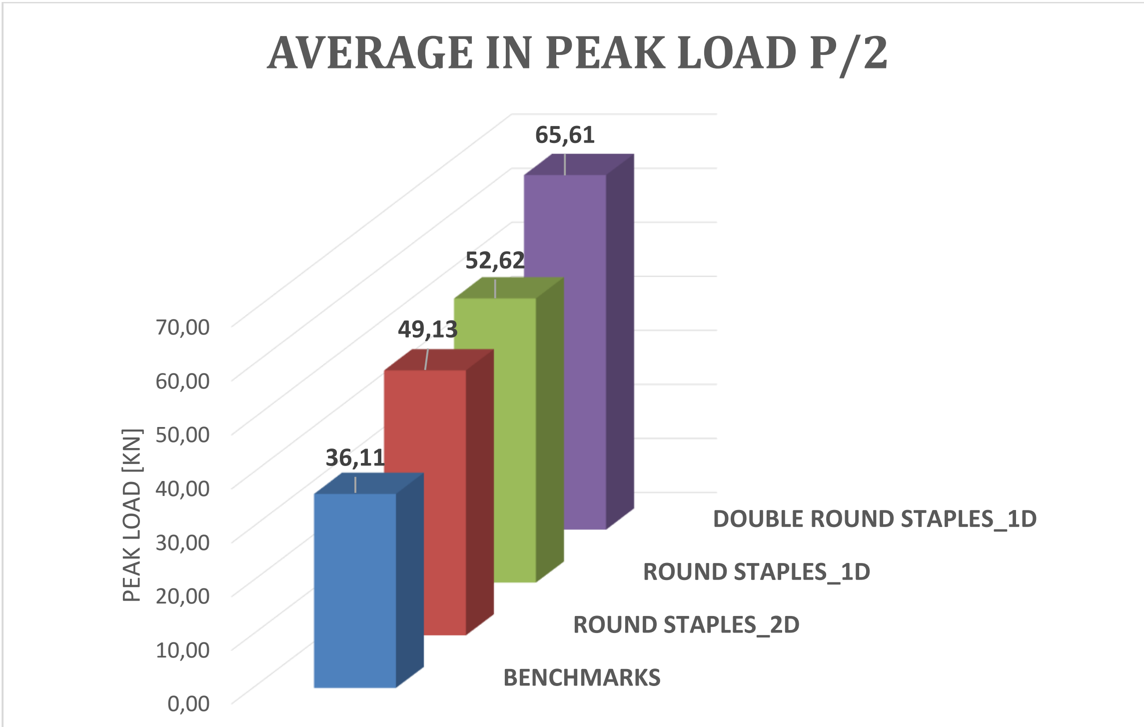

Figure 2.21 – Average in peak load between the round staples

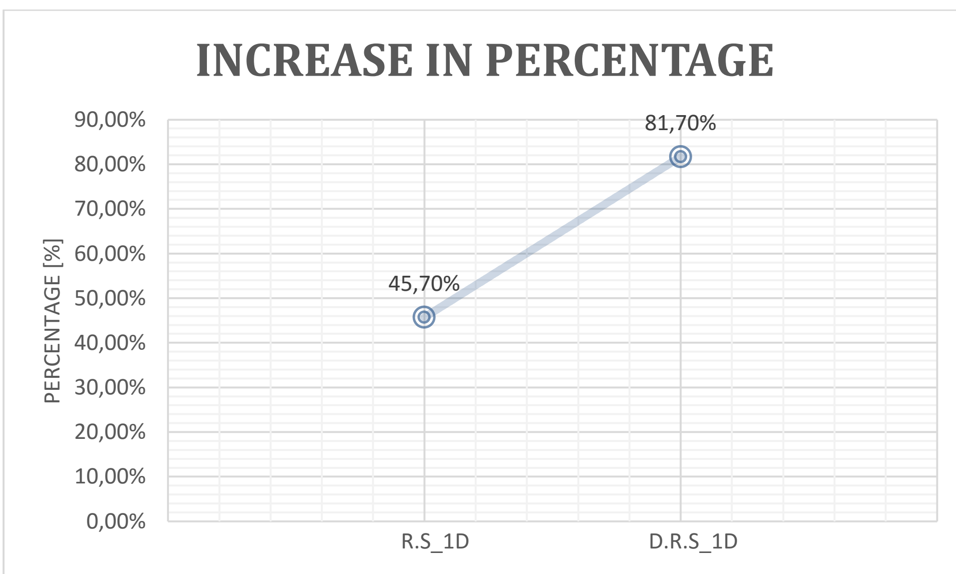

Figure 2.22 – Increase in percentage between the round staples

Since from the Fig 2.21, it seems strange how the 2-inches depth configuration could be less than the 1-inch depth, it is important to say that in the 2-inches depth only one specimen was run with the new round staple system. As it shown in the table 2.3 this only result is not sufficient to prove any rule and also this only result could be part of a minimum in a series of more specimens hypothetically run. In fact, the minimum value of the 1-inch depth is 46,34, which is less than 49,13. This is just a hypothesis, but it is enough to understand that also in this case, on increasing the depth, we don't reach any consistent and remarkable improvement.

2.3 FAILURE MODES ANALYSIS

During the tests, six main failure modes were observed.

This section wants to describe each type of rupture, analyzing case by case the reason, giving an interpretation and a potential understanding of what each failure means.

Below the main failure modes are summarized as letters:

A. Rupture as delamination of the CFRP sheet
B. Slippage of the CFRP sheet beneath the anchor, without their ruptures
C. Slippage of the CFRP sheet beneath the anchor, with the rupture of the CFRP sheet
D. Rupture of the anchor with the delamination of the CFRP
E. Rupture of the concrete substrate and rupture of the anchor
F. Rupture of the concrete substrate without the rupture of the anchor
G. Rupture of the CFRP sheet outside the bond area

Failure A - Rupture as delamination of the CFRP sheet

Figure 2.23 – Failure A

Only the benchmarks presented this type of failure. That is due to the fact that of the absence of an anchorage system. The failure mode A is a rupture by debonding of the CFRP sheet at the adhesive-to-concrete interface. Debonding initiated at the loaded end of the CFRP sheet and it brought propagated to the unloaded end.

The debonding caused the removal of the epoxy layer from the substrate and also a thin layer of concrete was noticed on the detached FRP sheet area.

The fig. 2.23 shows the typical type A failure.

Failure B - Slippage of the CFRP sheet beneath the anchor, without their ruptures

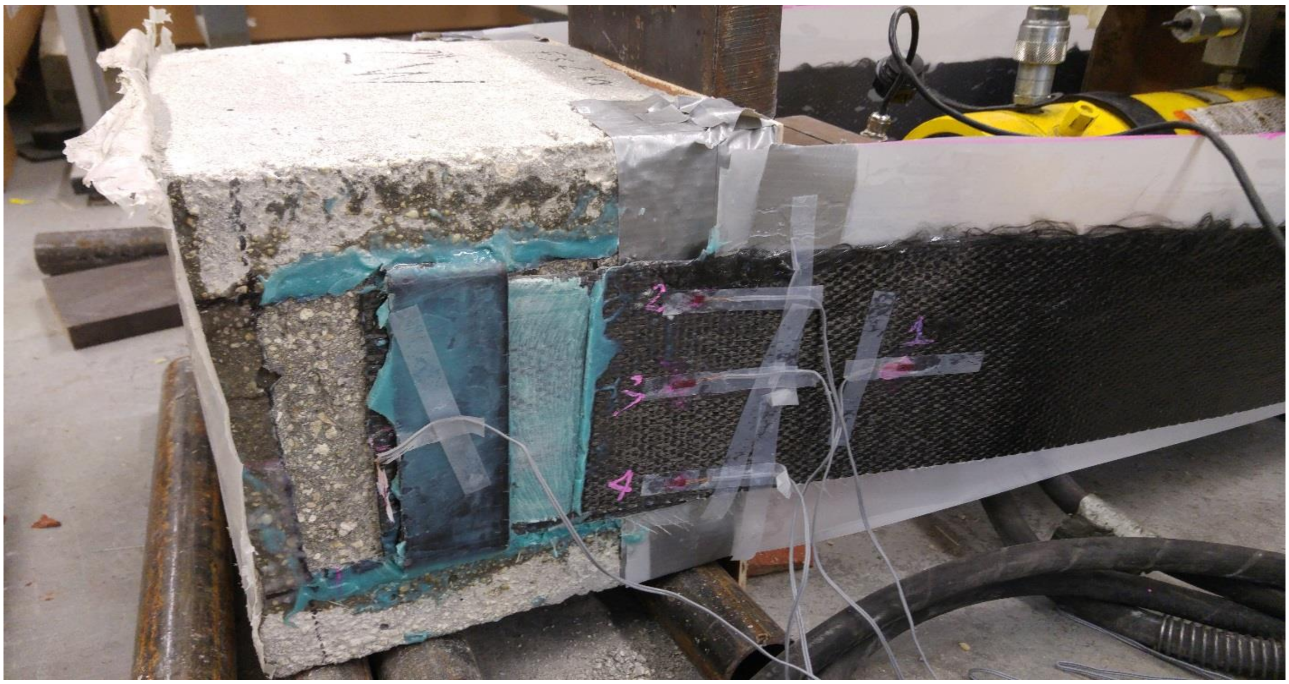

Figure 2.23 – Failure B

This type of failure is a particular one: It happened as a debonding of the CFRP sheet at the adhesive-to-concrete interface, followed literally by a slippage of the CFRP sheet beneath the anchor, as to mean an insufficient adhesive-to-concrete and anchor-to-CFRP interface. In fact, this failure mode is due to an insufficient quantitative of primer spread on the concrete surface first, and under the anchor area secondly.

Anyway, this failure mode is still ideal for determining the sufficiency of the anchor, since the strains across the width of the sheet monitored showed a good stress distribution with high values of the same

This failure mode was observed in only one anchored specimen. The above fig. 2.23 represents the failure mode B

Failure C - Slippage of the CFRP sheet beneath the anchor, with the rupture of the CFRP sheet

Figure 2.24 – Failure C

With the use of anchors, a CFRP sheet rupture failure reveals that the sheet has developed its full strength. The failure mode C is ideal for determining the sufficiency of the anchors and develop guidelines for anchor design. This rupture indicates the maximum tensile strength reached by the FRP-anchorage system, with a good anchor resistance.

However, there may be cases in which a sheet rupture does not indicate the development of full strength of the system. This can be understood by the strains reading. A good level of strains (usually values around a minimum of 0.6%, 0.7%) indicate the development of full strength of the system. The Fig. 2.24 represents the failure mode C.

After the propagation of the debonding cracks toward the anchor region, the enhanced strength of the anchored system was reached thanks to the remaining length of the bonded FRP sheet and the restraint provided by the anchor. The debonding started in the adhesive-to-concrete interface and the layer of primer was totally removed from the concrete surface at the end of the test.

Failure D - Rupture of the anchor with the delamination of the CFRP

The failure of the anchor indicates that anchors do not have sufficient capacity to develop the full strength of the CFRP sheet and is generally an undesirable failure mode. From previous studies, it has been stated that anchor failures depend on several factors as the size of the anchor, the force transfer mechanism between the sheet and anchor (bend radius and CFRP patches), and finally the adherence to installation procedures.

This type of failure was observed only for the round staple anchor, In particular, for the anchors that showed a greater embedded depth (2-inches depth). Especially, for all of them, the rupture happened on the bend radius, on the rounded corner side where the fibers were to change direction from the vertical to the horizontal plane.

The Fig. 2.25 shows the failure mode D

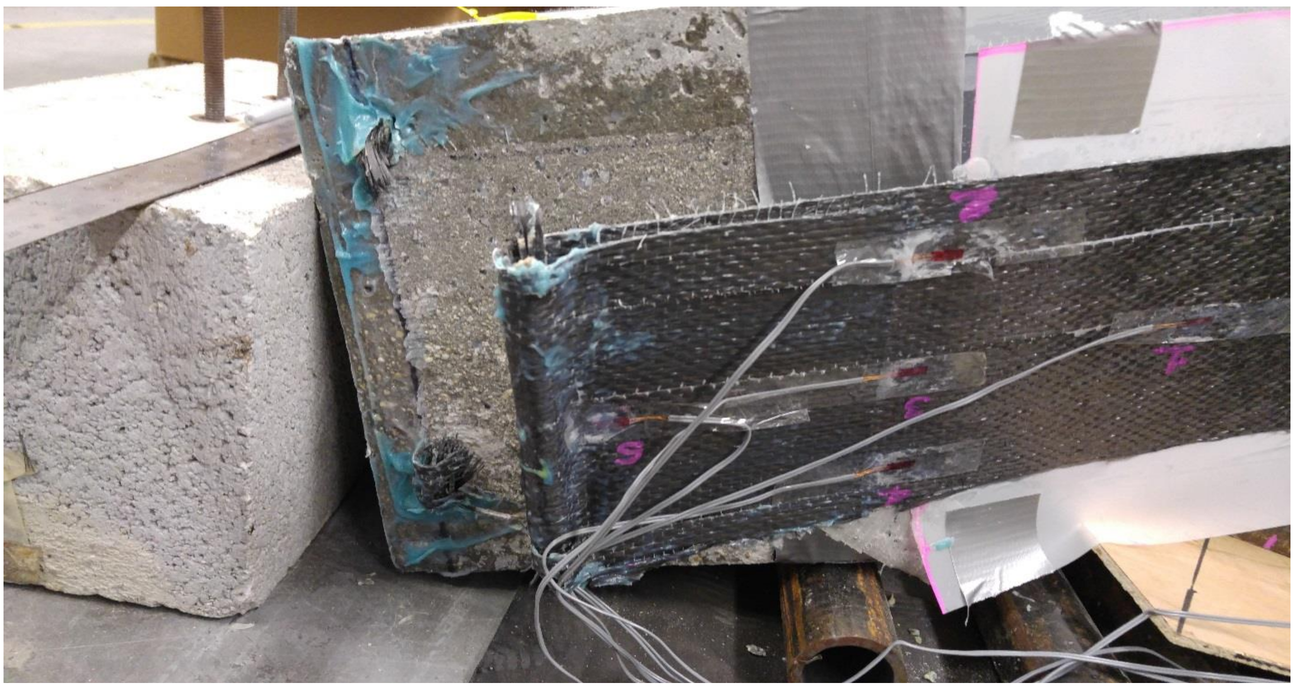

Figure 2.25 – Failure D

Failure E - Rupture of the anchor followed by the rupture of the concrete substrate

Again, the failure mode E was observed only in the specimens that were anchored with the round staple anchorage system. In this case, the rupture of the concrete always initiated first at one end, where the leg of the round staple was embedded; after this, immediately the opposite leg of the anchor took the entire stress, breaking again the anchor along the bend radius. The Fig. shows the failure mode E

Figure 2.26 – Failure E

Failure F - Rupture of the concrete substrate without the rupture of the anchor

Figure 2.27 – Failure F

The failure mode F was observed only in the specimens that were anchored with the flat staple anchorage system. In this case, the failure was due entirely to the rupture of the concrete substrate, as shown in the pictures (Fig. 2.27). Since the maximum shear capacity of the non-reinforced concrete was reached, the anchor was still performing well, assuming that it could have been achieved a higher load.

This rupture was fully observed in two of the 3-inches flat staple anchors and partially in two of the 2-inches flat staple anchors.

Failure G - Rupture of the CFRP sheet outside the bond area

The failure mode G was observed only in the specimens that were run for the test 1, with the old installation. This is the worst type of rupture because unfortunately, we can not obtain any interesting data from them.

The rupture did not occur on the bonded part, where the anchor was installed, but on the dry CFRP outside the bond area at a relatively low-stress level compared with the tensile strength of the CFRP itself. The Fig. 28 shows the failure mode G. This type of rupture is basically due to problems correlated with the installation process and the alignment of the system. In fact, the perfect alignment with the installation used for the test 1 was very hard to ensure and the specimens were found to be very sensitive to the handling operations.

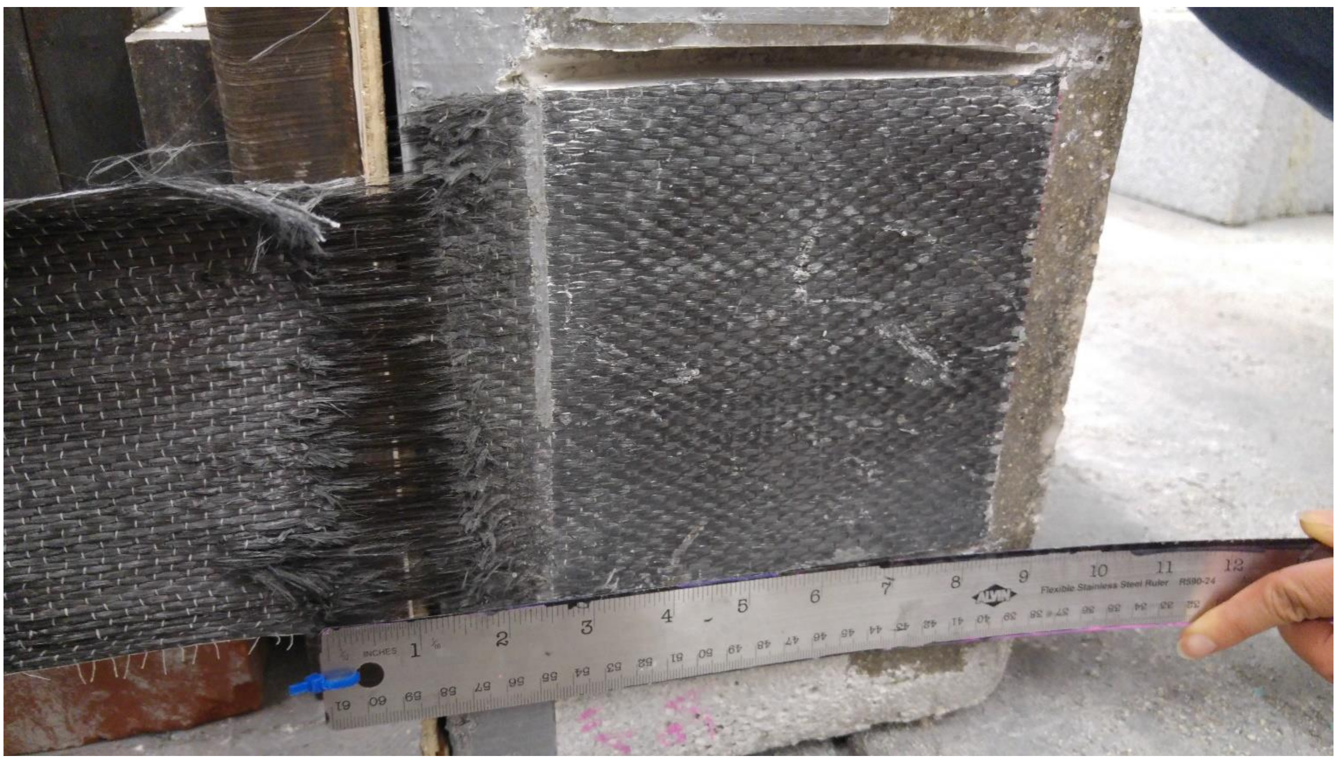

Figure 2.28 – Failure G

3. COMPARISONS

3.1 STAPLES VS SPIKE ANCHORS

In this section, a brief comparison between the performance of the staple anchors and the spike anchor system is provided in terms of peak load, strains distribution and type of rupture.

3.1.1 Peak load interpretation

Table 3.2 – Summary anchors peak loads

Anchor's type	Anchor's Configuration	Peak Load [KN]
Spike anchors	60 degrees fan opening 90 degrees fan opening	57,8 66,38
Flat staple anchors	1 in. width – 1 in. depth 2 in. width - 1 in. depth 3 in. width - 1 in. depth	57,35 62,21 66,42
Round staple anchors	Single conf. - 1 in. depth Double conf. - 1 in. depth	52,62 65,61

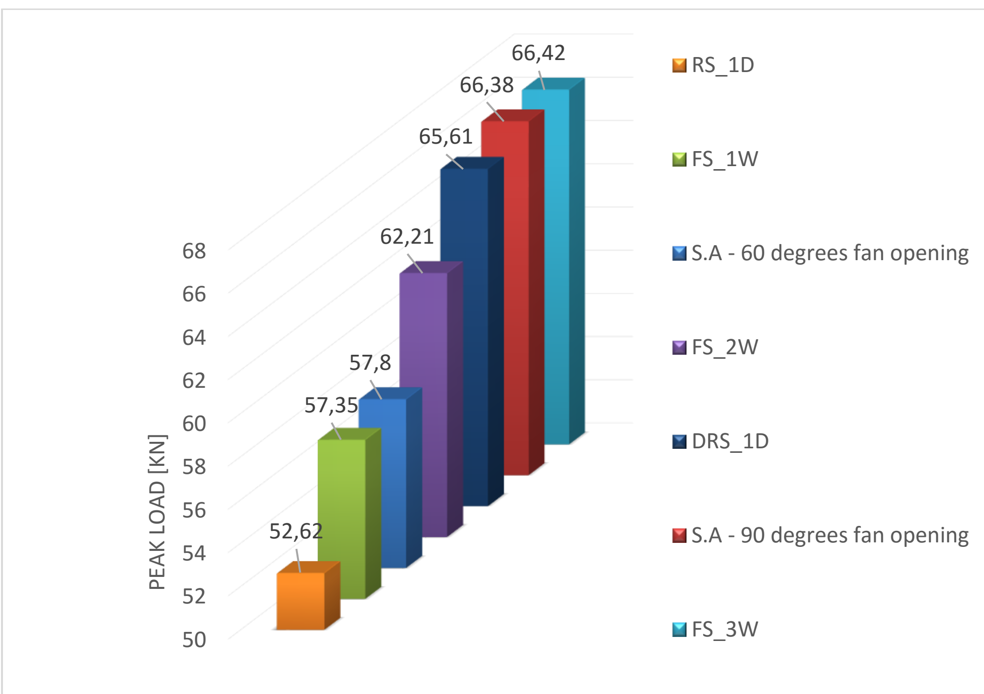

Figure 3.1- Comparisons staples-spikes peak loads in ascending order

Table 3.1 and Figure 3.1 present a comparison in terms of peak load between the spike anchors type and the staple anchorage system.

It is possible to clearly see how, for the flat staple anchorage system, the 1-inch width configuration perfectly resemble the 60 degrees fan opening, while the 3-inches width can be compared to the 90 degrees fan opening spike anchor (in terms of peak load). The 2-inches width, instead, it situates in between the two type, getting close mostly to the 3-inches configuration. This is due to the fact that each configuration presents a difference in terms of covered area. Obviously, the peak load increases at the increase of that covered area, which is the only variable between all the specimens.

Regarding the round staples, it is possible to notice a huge difference between the single configuration and the double configuration; in fact, the latter leads to an improvement of about 24,7% from the single round staple configuration. That is due to the fact that the double round staples seem to have a better splitting and bending control, giving to the 1st anchor located at the edge (the one in which the FRP laminate is wrapped around) the only task to resist and contrast the stresses. In this way, the 2nd extra anchor, positioned 3 inches far from the first one, beside taking part of the stresses, it controls mostly the stresses redistributing them better for the 1st anchor. Finally, another important reason of the big improvement is due to the fact that the effective contact area, in the case of the double round staple anchor configuration, it is doubled.

3.1.2 Strain interpretation

Since the covered surface is greater than the one covered by the spikes, without any doubts the staples anchor distribute better the stresses. In fact, for the spike anchors, the strain were concentrated in front of the anchor (and that covered area was not along the entire FRP sheet width). Our anchors, instead, they distribute better the strains over the entire area of the FRP, since they literally cover all the entire FRP laminate width fixed, in this study, at 6 inches. For this reason, in some cases, the spikes used to break only by the outside edges, while the staple anchors present other ruptures' types, as already discussed in chapter 2.3. Figures 3.2 and 3.3 show respectively the strain distributions along the 60 and 90 degrees configuration of the spike anchors.

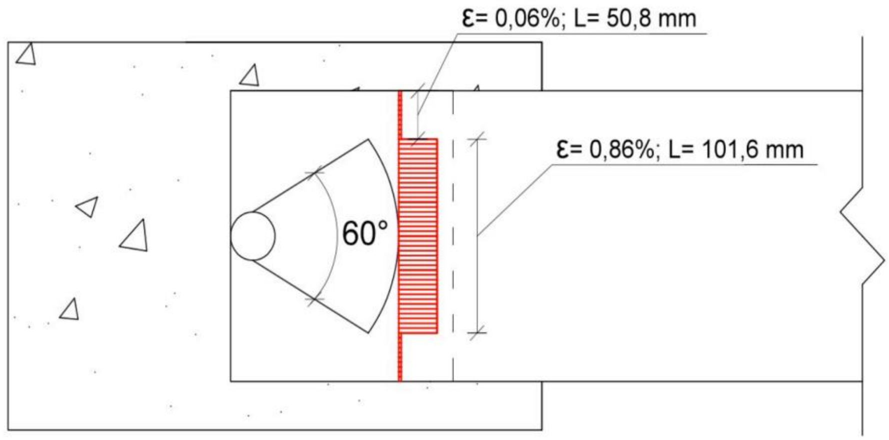

Figure 3.2- Strain distribution along the 60 degrees fan opening configuration of the spike anchorage system

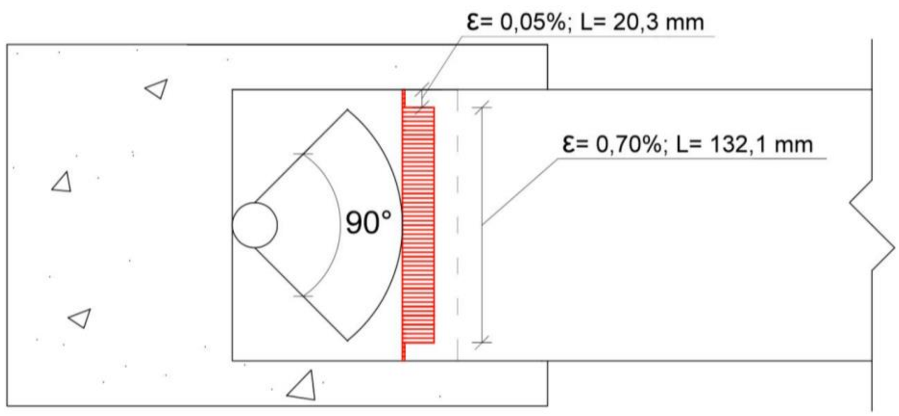

Figure 3.3- Strain distribution along the 90 degrees fan opening configuration of the spike anchorage system

Based on the data obtained from the test of the spikes anchors, run by Berneschi in 2015, the maximum value of strain was measured in front of the anchor in both the two specimens. In the case of 60° configuration specimens, this was greater than that measured in the 90° configuration specimens. Moreover, the strain recorded near the edge of the sheets (area not covered by the anchor) was always less than 0.1%. Based on this result, strain fields that develop in the FRP sheet appear to be not uniform in the transverse direction. For this reason, strains plotted longitudinally along the FRP sheet centerline are not representative of distributions near the edge of sheets and should be not taken as a design value. It is evidence that only sheet regions located within the anchor splay develop high stresses and strains. Due to the observations written above, a stress distribution model was supposed. It has the typical Gaussian distribution shape, symmetric with respect to the tension load. The following sketch in Fig. 3.4 illustrates the supposed strain distribution.

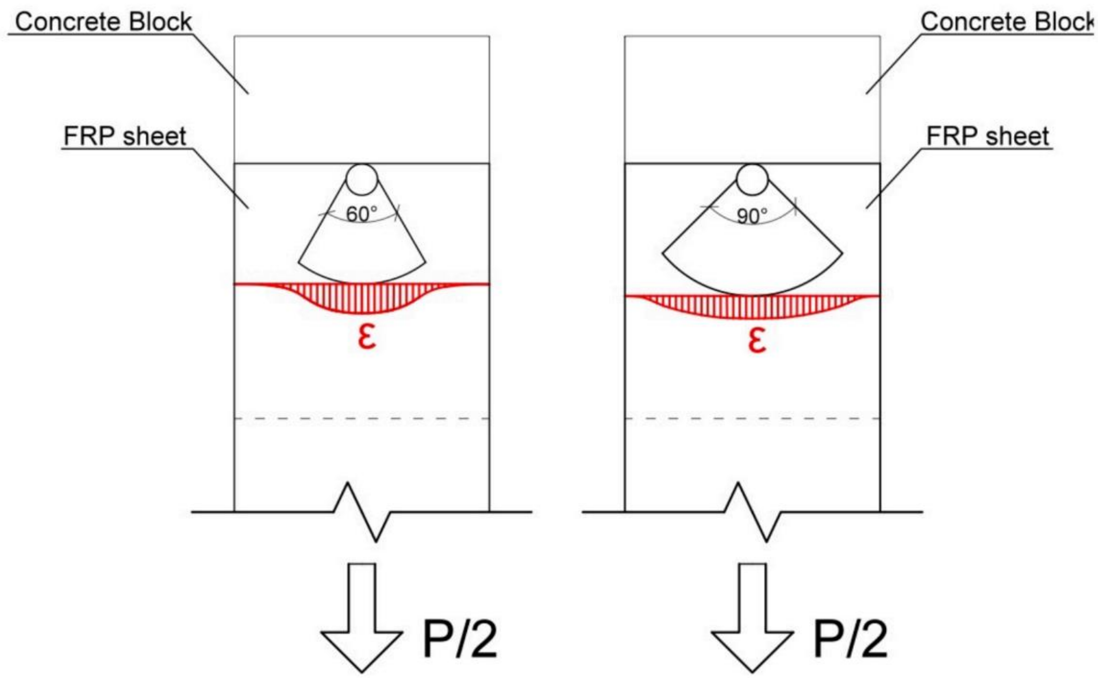

Figure 3.4 - Strain distribution model on the spike anchors (Berneschi, 2015)

3.1.2.1 Flat Staples

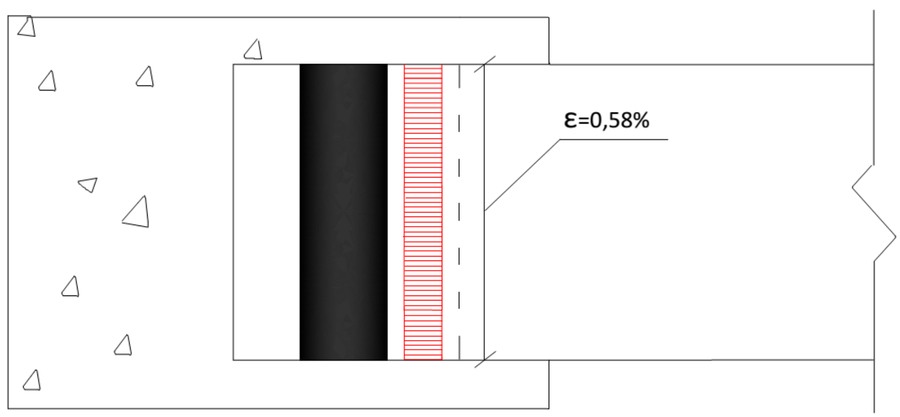

Figure 3.5 - Strain distribution along the 2-width flat staples

Figure 3.5 shows the typical strain distribution along the flat staples. This case is the one referred to the 2-width, with an average between the SG2, SG3 and SG4 (the strain gauges positioned just in front of the anchors) of $\varepsilon = 0{,}58\%$.

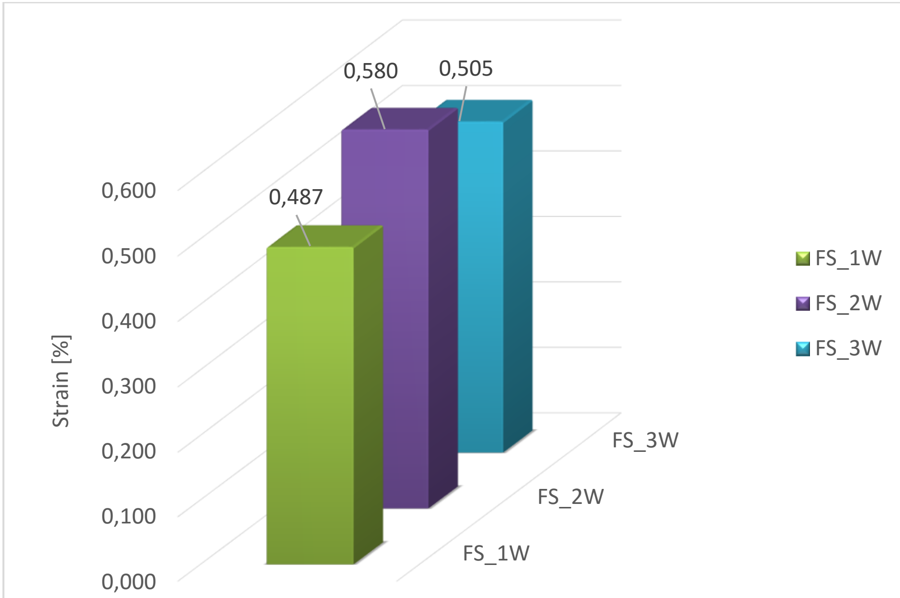

Figure 3.6 – Average of the strain distribution in front of the flat staple anchors for each configuration

Figure 3.6 shows the average of the SG2, SG3 and SG4 for the flat staples. We can observe a growth between the FS_1W and the FS_2W, while the FS_3W assumes a value which in between the previous ones. In this way, we can clearly identify the 2-width anchor as the one that is strong enough to develop the full capacity of the sheet.

3.1.2.2 Round staples

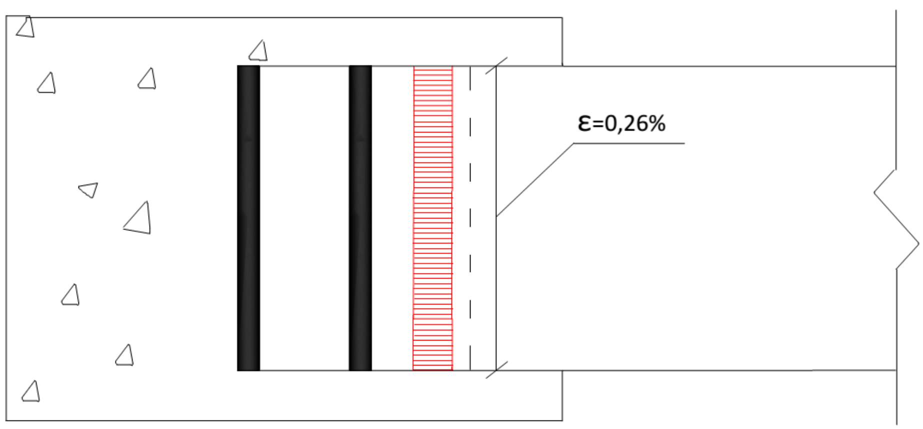

Figure 3.7 - Strain distribution along the double round staple anchorage system

The same applies to the strain distribution read from the round staples. As already explained, it is important to remind that in this case the strain gauges were installed on the second layer of the FRP sheet, wrapped around the first layer that is bonded to the concrete substrate. Figure 3.7 shows the strain distribution in front of the anchorage system for the double round staple configuration with an average value of about $\varepsilon = 0{,}26\%$.

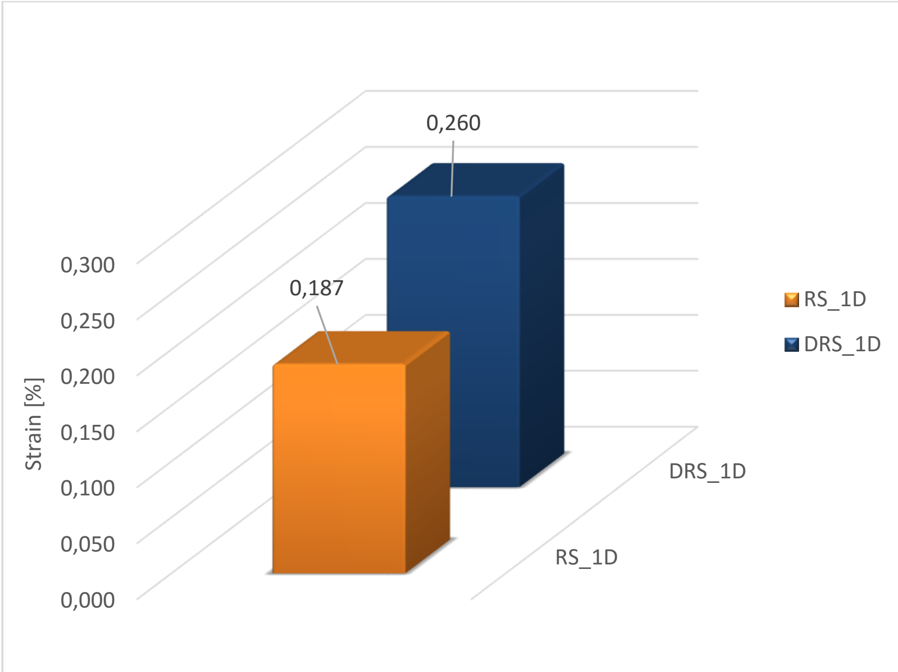

Figure 3.8 – Average of the strain distribution in front of the round staple anchors for each configuration

Again, Figure 3.8 illustrates the average of the strain gauges located in front of the anchors for the round staples. In this case, the increase is in ascending order from the RS_1D to the DRS_1D. Again, since the latter presents higher values of strains recorded, the double round staple configuration represents the case in which the anchors are strong enough to develop the full capacity of the sheet.

3.1.2.3 Theoretical peak load derived from the measured strains

Below, it is presented a correlation that connects the measured strains with the theoretical peak load. In fact, for each specimen, it can be calculated a theoretical peak load just by correlating the measured strains with the modulus of elasticity and the nominal area of the FRP laminate. The results refer only to the best discovered configurations of flat and round staple anchors (see chapter 2.2).

$$\sigma = E \cdot \varepsilon$$

$$\frac{P}{2}_{th} = \sigma \cdot A$$

σ is the nominal stress in the FRP sheet

E is the modulus of elasticity refereed to the wet FRP sheet and equal to 77,04

A is the nominal area of the FRP sheet: $A = 152{,}4\ mm^2$

$\frac{P}{2}_{th}$ is the theoretical peak load calculated from the strains read at the peak load

In this way for the two best configurations identified, we have that the theoretical peak load is:

$$\frac{P}{2_{th}} = 68{,}10\ KN$$

for the 2-width flat staple, while for the double round staple the theoretical peak load is:

$$\frac{P}{2_{th}} = 61{,}05\ KN$$

	E	ε	A	$P/2_{th}$	P/2	ΔP
	[Gpa]	[%]	[mm²]	[KN]	[KN]	[%]
Benchmark	77,04	0,4	152,4	46,96	36,11	30%
FS_2W	77,04	0,58	152,4	68,10	62,21	9%
DRS_1D	77,04	0,26	304,8	61,05	65,61	-7%

3.1.3 Types of failure modes

In this section, we discuss the failure modes in the anchored specimens provided with the spike anchors and with the staple anchors.

Regarding the spike anchors, three main type of ruptures were observed:

1. Adhesive-to-concrete interface debonding followed by rupture of the FRP sheet around the anchor
2. Adhesive-to-concrete interface debonding followed by slippage of the FRP sheet under the anchor
3. Failure at the concrete substrate

In the failure mode 1, the rupture of the fibers took place and started around the fan (on the uncovered area) that appeared still bonded to the FRP sheet after the failure, as shown in Fig. 3.9

Figure 3.9 – Failure mode 1, spike anchors

This first rupture mode was observed in the 60 degrees fan opening, where the covered area by the fan was smaller than the one covered by the 90 degrees configuration.

Rupture mode 2 was observed, instead, in the 90 degrees fan opening, where the initial debonding was in the adhesive-to-concrete interface and the primer was completely removed from the concrete surface. The final failure of the system was due to the slippage of the FRP sheet under the anchor. In this case, delamination between the fan and the FRP sheet was observed.

Also the failure mode 3, which is the failure of the concrete substrate, is typical of the 90 degrees fan opening.

Regarding the flat staples, as already analyzed in chapter 2.3, five different types of rupture were observed in the anchored specimens:

B. Slippage of the CFRP sheet beneath the anchor, without their ruptures
C. Slippage of the CFRP sheet beneath the anchor, with the rupture of the CFRP sheet
D. Rupture of the anchor with the delamination of the CFRP
E. Rupture of the concrete substrate and rupture of the anchor
F. Rupture of the concrete substrate without the rupture of the anchor

While failure modes B and C are typical of the staple anchorage system, the failure modes E and F can be correlated to the failure mode 3 observed in the spike anchors. At this point some considerations should be made:

Generally, a CFRP sheet rupture failure (failure mode 1 and 2 for the spikes and C for the staples) indicates that the sheet has developed its full strength. This failure mode is ideal for determining the sufficiency of the anchors and obtaining guidelines for anchor design, and for this reason is the desired failure mode. On the other hand, an anchor failure (failure mode D) indicates that anchors do not have enough capacity to develop the full strength of the CFRP laminate, representing an undesirable failure mode. In addition, failure modes E, F (for the staples) and 3 (for the spikes) show that the anchorage system-CFRP sheet is stronger than the concrete used to test the specimens.

3.2 RECOMMENDATION ON PRELIMINARY DESIGN PREVISIONS

Based on:

- Dispersion of the results (a low COV observed mainly in the 2-inches flat staple anchorage system).
- Type of rupture (the ideal failure mode is the failure mode C, which represents the full strength developed by the CFRP laminate).
- Strains interpretation (highest values of the strains are obviously preferred).
- Peak load significantly high.

We can say that the best configurations are:

- ➢ The 2-inches width, 1-inch depth anchor, for the flat staple anchorage system.
- ➢ The double round staple configuration, with 1-inch depth, for the round staple anchorage system.

In fact, only these two anchorage systems respect all the points previously explained in details. Regarding the flat staple anchorage system, it is important to underline that even if the 3-inches configuration reaches a higher value of peak load, that was too much. In fact, the 3-inches width anchor presented a break of the concrete (that was even a high strength concrete with around 59MPa of f'_c concrete compressive strength). The 2-inches width anchor, instead, presented a delamination with the rupture of the FRP, without the break of the anchor (in two cases that kind of rupture was combined with the rupture of the concrete substrate, which it pushes the 2-inches anchor to the limit of the usage). In this way, we can say that the 2-inches width anchor is strong enough, in order to achieve the full capacity of the FRP laminate.

Regarding the comparisons with the spikes anchors, the 2-inches anchor outclasses the 60 degrees fan opening in terms of peak load, strain interpretation and type of rupture (as shown in chapter 4). The 3-inches anchor performs a little better than the 90 degrees fan opening spike anchor, mostly in terms of strains. In fact, the big disadvantage of the spike anchors is that of not distribute the stresses evenly all along the FRP width. Regarding the round staples, the double round staple configuration is the preferred one. In fact, with an ideal rupture type and a uniform strain distribution it reaches high value of peak loads (in between the 2-inches and the 3-inches flat staple anchors).

4. RECOMMENDATIONS FOR FUTURE STUDIES

For future works, more studies should be done with different configurations of depth, even if the 1’’ depth is an ideal depth for a main reasons: the rebars interaction. Since most of the worldwide regulations gives some minimum requirements for the concrete cover (see table 4.1), a 1’’ depth, while anchoring an FRP reinforcement, would not be a problem of interact and damage the internal reinforcement of a slab.

Table 4.1 – Summary of the most common concrete cover requirements

Country	Concrete Code	Range of Concrete Cover (mm)
UK	BS:8110	25-50
EU	EN 1992 (EC2)	diameter +10 - 55
USA	ACI:318	40-50
Australia	AS:3600	15-78

Note: 1 inch (= 25.4 mm)

Also, from the results obtained in this research, tests on beams should be done, using the following set-up:

- One anchor 2-inches width, 1-inch depth on each end, on a 6” FRP sheet width.
- A double round staple configuration, 1-inch depth on each end, always on a 6” FRP sheet – width.

Note: It would be good to use the same width of the FRP sheet used in all the shear test (6” width).

5. CONCLUSIONS

The research presented in this report represents an initial study of the interaction between the staple anchors and FRP laminates. Since the anchors are more subjected to shear forces rather than pullout forces, an experimental campaign through shear tests has been developed in order to fully understand the behavior of this anchorage system. From the main test (test 2) run it has been obtained a full understanding of the improvement on the global strengthening system by modifying different parameters of this anchor system.

In this report, we made also a comparison between the staple anchorage system and one of the most used and efficient, so far, anchor system (spikes anchors) for carbon fibers reinforced polymer.